

https://dspace.org/

Mineralogy and geochemistry of the impact breccias of the Bosumtwi impact structure, Ghana : genesis and secondary proccesses

Coney, Louise

2009-05-28T10:56:53Z
http://hdl.handle.net/10539/6991

Downloaded from a DSpace repository. https://dspace.org/

The Meteoritical Society

Meteoritics & Planetary Science 42, Nr 4/5, 667–688 (2007)
Abstract available online at http://meteoritics.org

Geochemistry of impactites and basement lithologies from ICDP borehole LB-07A, Bosumtwi impact structure, Ghana

Louise CONEY[1*], Wolf Uwe REIMOLD[1, 2], Roger L. GIBSON[1], and Christian KOEBERL[3]

[1]Impact Cratering Research Group, School of Geosciences, University of the Witwatersrand, Private Bag 3, P.O. WITS, Johannesburg 2050, South Africa
[2]Museum for Natural History (Mineralogy), Humboldt University, Berlin, Invalidenstrasse 43, D-10115 Berlin, Germany
[3]Department of Geological Sciences, University of Vienna, Althanstrasse14, A-1090 Vienna, Austria
[*]Corresponding author. E-mail: ConeyL@science.pg.wits.ac.za

(Received 13 October 2006; revision accepted 01 January 2007)

Abstract–In 2004, a drilling project by the International Continental Scientific Drilling Program (ICDP) at the Bosumtwi impact crater, Ghana (1.07 Myr old and 10.5 km in diameter), obtained drill core LB-07A, which sampled impactites and underlying metasediments in the crater moat surrounding the small central uplift of the structure. The LB-07A core consists of three sequences: 82.29 m of an upper impactite sequence of alternating polymict lithic and suevitic impact breccias overlying 54.88 m of so-called lower impactite of monomict impact breccia with several suevite intercalations, and 74.53 m of meta-graywacke and altered shale of the basement, also containing a number of suevite intercalations. Major- and trace-element characteristics of all three sequences have been determined to investigate breccia formation and the role of the respective basement lithologies therein. Compositions of polymict impact breccias of the crater fill revealed by core LB-07A are compared with the compositions of the Ivory Coast tektites and the fallout suevites. The impactites of the LB-07A borehole appear well homogenized with respect to the silicate component, and little change in the ranges of many major- and trace-element differences is seen along the length of the borehole (except for Fe_2O_3, MgO, and CaO contents). Much scatter is observed for a number of elements, and in many cases this increases with depth. It is proposed that any variability in composition is likely the function of clast population differences (i.e., also of relatively small sample sizes). No systematic compositional difference between polymict lithic and suevitic impact breccias is evident. An indication of carbonate enrichment due to hydrothermal alteration is observed in samples from all lithologies. The impactites of the borehole generally show intermediate compositions to previously defined target rocks. The fallout suevites have comparable major element abundances, except for relatively lower MgO contents. The Ivory Coast tektites are generally similar in composition to the LB-07A suevites, but broader ranges in MgO and CaO contents are observed for the LB-07A suevites.

INTRODUCTION

The Bosumtwi structure in Ghana, West Africa, is a complex impact crater that is 1.07 Myr old (Koeberl and Reimold 2005). It is linked to one of only four known tektite and microtektite strewn fields (the Ivory Coast strewn field) (e.g., Glass et al. 1991; Koeberl et al. 1997). The young crater structure is well preserved. The recent drilling project by the International Continental Scientific Drilling Program (ICDP) (Koeberl et al. 2005, 2006) resulted in the recovery of rocks of the deep crater moat and from the flank of the small central uplift (drill cores LB-07A and LB-8A, respectively) (e.g., Coney et al. 2007; Ferrière et al. 2007a). This includes impact breccias as well as basement lithologies (for petrographic details see Fig. 5 of Coney et al. 2007). Stratigraphic details for these drill cores are presented in Fig. 4 of Coney et al. (2007) and Fig. 2 in Ferrière et al. (2007a). Results of macroscopic drill core description, as well as hand specimen and microscopic analysis of our sample suite from the LB-07A borehole, are discussed by Coney et al. (2007). Here we present first geochemical results for this impactite sample suite and the underlying crater basement. This allows comparison with the results of previous geochemical studies (Koeberl et al. 1998; Boamah and Koeberl 2002, 2003, 2006; Dai et al. 2005) that focused on rocks sampled around and beyond the crater rim, and also with the composition of

© The Meteoritical Society, 2007. Printed in USA.

samples from core LB-08A into the flank of the central uplift (Ferrière et al. 2007b) and with Ivory Coast tektites and microtektites (Koeberl et al. 1997, 1998).

REGIONAL GEOLOGY: A BRIEF OVERVIEW

The ~2.1–2.2 Gyr old Birimian Supergroup (Wright et al. 1985; Leube et al. 1990; Davis et al. 1994; Hirdes et al. 1996; Oberthür et al. 1998) in which the Bosumtwi impact structure was excavated consists of a variety of metasediments (traditionally regarded as Lower Birimian) and metavolcanics (Upper Birimian). However, no age difference is apparent between the two units, and thus it has been recommended (e.g., Leube et al. 1990) that the subdivision between Upper and Lower Birimian be abandoned. The metasediments comprise interbedded phyllites, schists, meta-tuffs, meta-graywackes, shales, and slates. There are a number of different varieties of meta-graywacke, some of which are quartz-rich (metas-andstones and quartzite) or carbonate-rich. Metavolcanic rocks occur to the southeast of the crater and includes altered basic intrusives with intercalated metasediments. To the east and southeast of the crater, clastic sedimentary rocks thought to represent the detritus of the eroded Birimian Supergroup (Leube et al. 1990) occur and are known as the Tarkwaian Group (see Fig. 3 in Coney et al. 2007). A number of granitic and mafic intrusions occur throughout the region (see Koeberl and Reimold 2005 and Karikari et al. 2007 for further details). The crater structure is largely covered by Lake Bosumtwi, which is 8.5 km wide.

PREVIOUS GEOCHEMICAL WORK

One main focus of geochemical work on the Bosumtwi impact structure in previous years has been to establish the link between the impact structure and the Ivory Coast tektite strewn field (first described by Lacroix 1934). The tektite strewn field and the crater have been correlated on the basis of geochemical composition (e.g., Schnetzler et al. 1966, 1967; Kolbe et al. 1967; Shaw and Wasserburg 1982; Jones 1985; Koeberl et al. 1998) and age (e.g., Gentner et al. 1967; Koeberl et al. 1997).

Koeberl et al. (1998) identified, by major- and trace-element chemical analysis and petrographic studies, four main target-rock groups: phyllite-graywacke, granite dikes, shale, and Pepiakese granite. They found that the distinction between phyllites and graywackes was not well defined, and so included them in one group. The phyllite and graywacke samples studied by Koeberl et al. (1998) have variable chemical compositions, but are distinct from the shales in that they have higher silica and lower alumina, iron, and magnesium contents. Koeberl et al. (1998) also found that the regional granitoids represent two different chemical types. The granite dikes are relatively unaltered in comparison to the Pepiakese granite, which forms an intrusive granitoid body on the northeastern side of Lake Bosumtwi (Fig. 3 in Coney et al. 2007). The Pepiakese granite also contains more amphibole and biotite than the other granitoids sampled. The Pepiakese granite samples in general have high but variable Fe, Mg, and Ca contents (thought to have been caused by extensive chloritization and the presence of the mafic minerals).

Additionally, Koeberl et al. (1998) analyzed a number of the rocks from around the Bosumtwi crater structure for their O, Sr, and Nd isotopic compositions. The Rb-Sr isotopic ratios measured for selected target rocks were similar to those previously obtained for the Birimian granitoid intrusions (Taylor et al. 1992). Taylor et al. (1992) used the Rb-Sr, Sm-Nd, and Pb-Pb isotopic systems to constrain the rock-forming events, and found that the results from the various isotope systems were generally in agreement with each other and that the Birimian magmatic crust-forming event took place from ~2.3 to 2.0 Gyr by differentiation from slightly depleted crust. The isotopic data of Shaw and Wasserburg (1982) and Koeberl et al. (1998) supported the interpretation that the Ivory Coast tektites were similar in composition to the rocks exposed at the Bosumtwi impact structure, indicating that they both formed during the same event (Koeberl et al. 1998).

A strong airborne radiometric anomaly was found around and to the north of the crater rim by Plado et al. (2000). To examine the hypothesis that the signal was caused by local enrichment of potassium, Boamah and Koeberl (2002) measured major- and trace- element concentrations of a number of soil samples from around the Bosumtwi structure. They found that the soil samples showed considerable variation relative to the parent rocks from which they had been derived (but within the range obtained for the source rocks). Boamah and Koeberl (2002) concluded that the variable geochemical signature reflected the extensive chemical weathering that had taken place in the tropical environment. Boamah and Koeberl (2002) suggested that the strong anomaly could have been caused by potassium mobilization owing to the impact event, or to the local presence of source rocks with variable potassium concentrations.

Boamah and Koeberl (2003) reported on a shallow drilling program to the north of the crater rim, where extensive suevite occurrences were known to occur (first mentioned by Junner 1937), in order to determine the thickness of the suevitic ejecta blanket in several locations, as well as to determine geochemical characteristics of the ejecta in an attempt to link the aero-radiometry data with ground-based analyses. They found that the major- and trace-element concentrations of the suevites were similar to those of the target rocks in the area and noted that the metasedimentary target rocks and the granite dikes provided an important contribution to the fallout suevites, together with a lesser proportion of Pepiakese granite. This is in contrast to the composition of fallback suevites found in the drill cores within the crater fill (see petrographic data of Coney et al.

2007 and Ferrière et al. 2007a), in which granitic components are only a minor contributor. The regional geological observations by Reimold et al. (1998) suggested that only some 2% of the target was composed of granite.

The possible presence of a meteoritic component in tektites and impact breccias and the indigenous siderophile element component of the target rocks were investigated by a number of workers (Palme et al. 1978; Jones 1985; Koeberl and Shirey 1993; Dai et al. 2005). Koeberl and Shirey (1993) measured the concentrations and isotopic ratios of osmium and rhenium for a number of Ivory Coast tektite samples as well as for country rocks from the Bosumtwi structure. The osmium isotopic ratios of the tektites are close to meteoritic values, whereas the rocks of the Bosumtwi structure showed values rather typical of older continental crust. Koeberl and Shirey (1993) concluded that the Re-Os isotopic signatures of the tektites provided unambiguous evidence for contamination with 0.1–0.6 wt% meteoritic component. However, no clear meteoritic component could be distinguished in the fallout suevites (Dai et al. 2005) because of the high siderophile element contents in the target rocks (see also McDonald et al. 2007, on PGE abundances).

METHODOLOGY

In order to examine the compositions of the LB-07A impactites, their possible source rocks, the mixing of target rocks in formation of the impact breccias, and the possible presence of a meteoritic projectile, a suite of 86 samples was subjected to geochemical analysis. Core samples 5–10 cm in length (quarter cores with a radius of 3 cm) were crushed and powdered. Twenty-three polymict lithic breccia, 36 suevitic breccia, 13 monomict impact breccia, and 14 metasediment samples from the basement to the crater structure were analyzed. The samples were first crushed and milled to a powder (after pre-contamination of crushing instruments). Eighty-six samples were milled in tungsten carbide swing mills, or, where possible, in an agate mill, in order to avoid contamination (from the equipment). The powders were analyzed for major- and trace-element concentrations using standard X-ray fluorescence (XRF) procedures at the University of the Witwatersrand, Johannesburg (see Reimold et al. 1994 for details on the procedures, precision, and accuracy) and Humboldt University, Berlin (see Schmitt et al. 2004 for details on the procedures, precision, and accuracy). Trace-element concentrations were determined on 200 mg aliquots by instrumental neutron activation analysis (INAA) at the University of Vienna, Austria, following procedures described by Koeberl (1993, 1994). In those cases where values were obtained by both XRF and INAA for the same element, these were compared and generally found to be in agreement; consequently, averages of both the XRF and INAA sata, or only XRF values are reported here for these samples.

LITHOSTRATIGRAPHY OF THE LB-07A DRILL CORE

Detailed lithostratigraphic studies of core LB-07A are reported by Coney et al. (2007), based on the same sample suite that was analyzed geochemically. The LB-07A core was drilled from a depth of 333.38 m to a depth of 545.08 m below lake level and consists of ~137 m of impactites and ~75 m of crater basement. The impactites are divided into an upper (333.38–415.67 m in depth) and a lower (415.67–470.55 m in depth) sequence. The upper and lower impactites differ from each other in that the upper impactites are polymict, whereas the lower ones are monomict. The upper impactites consist of three polymict lithic breccia units alternating with three suevite units (see Fig. 4 in Coney et al. 2007). The breccias are dominated by meta-graywacke and shale (some of it graphitic) clasts, plus minor phyllite, mica-schist, and quartzite, and traces of primary carbonate. The lithic breccias and suevites are very similar in terms of clast types and size ranges, as well as shock deformation of clasts, and the lithic breccias differ from the suevites only in the absence of melt particles (Coney et al. 2007). Clast size is variable: subcentimeter- to decimeter-size clasts have been observed (see Coney et al. 2007). The melt particles in the suevites are angular to rounded, either mafic (brown-black) or felsic (colorless to white), and the matrices of the suevites are gray-brown in color. The abundances of the melt particles vary between 1.5 and 7 vol%.

The lower impactites consist of monomict breccias, dominated by meta-graywacke, with minor shale and two thin suevite intercalations. The highest proportion of melt in the borehole is found in the suevites in this interval (~18 vol%–but in potentially nonrepresentative samples as discussed by Coney et al. 2007), and the melt particles differ in color from the melt particles of the upper impactites in that they are greenish yellow (as is the matrix of the suevites). This is attributed to a higher degree of alteration in the lower impactites.

The basement rocks, intersected in the interval from 470.55–545.08 m, consist of highly altered shales with altered remnants of graphitic schist, alternating with meta-graywacke. Two suevite intercalations and a single hydrothermally altered granophyric lithology are found within the basement rocks. The upper suevite (483.00 m) is characterized by a dense gray-black matrix and the lower one (513.90 m) by a light gray matrix. The meta-graywacke and shales (including the graphitic schist) are locally strongly laminated and tightly intercalated, also with thin bands of quartzite, metasandstone, and carbonate bands. Given the extensive alteration of the lower levels of the core, it is likely that some of our relatively small samples represent mixtures of such lithologies, which could cause local variation in chemical composition (for example, with regard to CaO and loss on ignition [LOI] contents; see below).

Evidence for hydrothermal alteration is present in the form of a number of cross-cutting quartz and carbonate veins (both macroscopic and microscopic), as well as carbonate pods (up to 10 cm in size) in the impactite sequence. The alteration is most pronounced in the upper impactites, together with the suevites of the lower impactites, with less evidence observed in the monomict breccias (though the core is highly disaggregated and these features may not be preserved). Within the basement rocks, carbonate pods up to 10 cm in width are observed, and secondary sulfide network patches have been identified microscopically by Coney et al. (2007).

The lithostratigraphic subdivisions identified by Coney et al. (2007) are used below to examine whether any substantial changes in the major- and trace-element signatures exist within borehole LB-07A. The XRF and INAA results are presented in Table 1.

MAJOR ELEMENT COMPOSITIONS

The major-element profiles, plotted against depth in order to investigate the respective compositions of the different lithologies, are shown in Fig. 1. Table 2 gives the overall ranges in the major elements for the various lithologies. The abundances of MnO and P_2O_5 have similar patterns, and as these elements form minor components of the total major element signature, these data are not discussed in detail here.

Polymict Lithic Breccias

The polymict lithic breccias have SiO_2, TiO_2, and K_2O contents within small ranges, with only few outliers (see Table 2). The Al_2O_3 contents show a fair amount of scatter. The CaO contents vary mainly between 0.76 and 2.89 wt%, with a maximum of 8.59 wt%. Interestingly, Na_2O contents were found to be highest at the top of the core (and to decrease with depth) and vary between 0.94 and 3.78 wt%. The Fe_2O_3 (all Fe calculated as Fe^{3+}) contents vary between 3.26 and 7.53 wt%, and positively correlate with MgO values (between 1.5 and 15.0 wt%).

Suevites of the Core LB-07A

Most of the SiO_2 values of suevite samples range from 53.7 to 66.2 wt%, which is similar to that of the lithic breccias, although a few more siliceous suevite samples (up to 70 wt%) are in evidence. The TiO_2, K_2O, and Fe_2O_3 contents vary within similar ranges to those of the lithic breccias. The highest Fe_2O_3 values could not be correlated with high shale contents, so it is clear that another component is controlling the Fe_2O_3 composition, such as the sulfide or mica content variation. MgO contents are again correlated positively to the Fe_2O_3 contents. The Al_2O_3 values range from 12.44 to 17.04 wt%, with a single outlier at 5.02 wt% (within a sample of high carbonate content). The CaO contents are highly variable and the full range is between 0.95 and 10.06 wt%, with most values lying in the range of 0.95–2.89 wt%, which is comparable to the values observed for the lithic breccias. The Na_2O abundance varies between 0.11 and 5.38 wt%, with most values falling into the range of 0.11 to 3.71 wt%. It is most likely that these fluctuations are related to the feldspar minerals, which vary in abundance between 0.7 and 8.5 vol% in the suevites (see Coney et al. 2007).

Monomict Breccias

In the monomict breccias (lower impactites), SiO_2 varies between 56.01 and 76.95 wt%, which is a slightly wider range than that for the average polymict breccias of the upper impactites. K_2O and TiO_2 values are similar to those observed for the upper impactites. The Al_2O_3 contents vary between 10.9 and 18.96 wt%, which is the same range as observed for the basement lithologies (see below), but a smaller range than that seen for the suevites and lithic breccias. As with the other lithologies, CaO contents show extensive variation—mostly from 0.82 to 2.10 wt%, to a maximum value of 6.48 wt%. The Fe_2O_3 abundances show the most scatter out of all the lithologies. The Na_2O and MgO contents vary within a much smaller range than seen in the polymict breccias.

Basement Lithologies

In the basement rocks, the SiO_2 as well as K_2O contents vary within significantly larger ranges than those for the impactites; however, the bulk of the values are similar to those for the impactites. No correlation of K_2O contents with LOI values exists, which indicates that a significant proportion of CaO must be responsible for the high LOI values. The CaO contents vary between 0.39 and 8.49 wt%, similar to the overall range in the other lithologies. The altered shales have lower SiO_2, Al_2O_3, Na_2O, and P_2O_5, and higher Fe_2O_3, MnO, MgO, and K_2O contents than the meta-graywackes (Table 1). This agrees with the observations made by Koeberl et al. (1998).

Granophyric-Textured Lithology

The granophyric-textured lithology occurring at a depth of 487.12 m has a distinct chemical signature. It has low SiO_2, Na_2O, and K_2O abundances together with notably high CaO (6.16 wt%, correlated with a high LOI of 12.30 wt%) (Fig. 2), Fe_2O_3, and MgO contents, in comparison to the overall major element compositions of the basement rocks. The Al_2O_3 and TiO_2 contents are within the overall ranges observed for the basement lithologies.

Table 1. Major- (wt%) and trace-element (ppm, unless indicated otherwise) data for samples from the LB-07A borehole.

Sample no.	KR7-54[a]	KR7-1	KR7-55[a]	KR7-57[a]	KR7-56[a]	KR7-2	KR7-58[a]	KR7-3	KR7-59[a]	KR7-60[a]	KR7-4	KR7-62[a]	KR7-61[a]	KR7-34	KR7-5	KR7-63[a]
Depth (m)	334.48	334.91	336.52	336.81	337.80	339.22	342.2	346.66	347.16	352.91	353.16	355.02	355.05	355.72	356.61	357.45
Lithology	LB	LB	LB	LB	LB	LB	LB	LB	LB	LB	LB	LB	LB	LB	LB	LB
SiO_2	61.9	66.2	60.4	63.9	63.1	56.3	64.1	63.5	62.4	62.5	64.1	62.4	63.9	58.1	63.5	63.3
TiO_2	0.58	0.51	0.66	0.53	0.33	0.65	0.57	0.56	0.56	0.57	0.62	0.61	0.57	0.60	0.65	0.63
Al_2O_3	16.0	15.6	17.7	15.6	11.2	17.2	16.1	17.0	17.1	16.7	16.8	17.1	16.4	15.0	16.6	15.7
Fe_2O_3	6.28	5.18	6.79	5.64	3.26	6.94	5.74	5.64	6.40	6.15	6.17	6.40	6.12	6.69	6.23	5.45
MnO	0.06	0.04	0.05	0.05	0.08	0.05	0.05	0.05	0.05	0.05	0.04	0.04	0.04	0.07	0.05	0.05
MgO	3.48	1.65	2.83	2.31	1.47	2.46	2.45	1.88	2.42	2.55	2.59	2.57	2.51	5.19	3.13	2.26
CaO	2.00	1.13	2.03	1.78	8.59	0.98	1.79	1.34	1.47	1.76	1.33	1.39	1.47	2.89	0.76	2.48
Na_2O	2.79	3.02	2.56	2.69	3.30	1.71	2.70	2.56	2.69	2.66	1.91	2.70	2.69	3.04	2.95	3.33
K_2O	1.87	1.79	2.46	2.14	0.83	2.18	2.08	1.91	2.33	2.22	1.85	2.34	2.19	1.57	2.24	1.83
P_2O_5	0.10	0.09	0.10	0.09	0.05	0.10	0.10	0.10	0.13	0.11	0.12	0.11	0.09	0.12	0.10	0.12
LOI	4.40	3.64	4.10	4.20	7.70	11.8	4.00	4.27	4.00	3.90	3.80	3.90	3.80	6.49	4.02	4.30
SO_3	0.2		0.3	0.2	<0.1		<0.1		0.1	0.1		0.1	<0.1			0.3
Total	99.7	98.9	99.9	99.1	99.9	100.3	99.7	98.8	99.7	99.6	100.5	99.7	99.8	99.7	100.2	99.8
Sc	16.0	12.4	17.2	14.6	7.28	18.6	13.8	13.9	17.3	15.4	15.4	16.3	14.9	18.1	16.7	13.7
V	118	103	141	113	68	164	115	116	120	123	122	123	117	134	135	107
Cr	159	104	101	92	62	150	97	117	87.7	97	135	98	97	284	128	78
Co	19.5	10.8	18.5	20.0	6.79	18.7	15.9	13.8	17.2.	17.6	15.4	19.4	18.3	23.0	16.0	14.7
Ni	109	33	67	42	b.d.l.	58	50	44	39	57	52	49	42	94	41	28
Cu	58	20	58	51	33	40	39	30	40	59	27	50	42	32	24	42
Zn	83	61	84	76	36	89	73	64	87	81	73	84	81	79	80	73
As	12.4	1.50	7.12	8.42	3.35	<1.1	11.1	6.31	1.38	23.9	8.75	7.56	9.25	7.19	0.16	5.08
Se	<2.2	0.10	<2.4	<2.2	<1.4	0.22	<2.1	0.11	<2.5	<2.68	0.21	<2.7	<2.6	0.18	0.16	<2.5
Br	0.6	<0.4	0.5	0.5	0.4	<0.4	0.3	<0.3	0.6	0.3	0.39	0.5	0.5	<1.2	<0.4	0.5
Rb	65	68	92	80	31	92	76	70	90	85	75	91	84	68	95	70
Sr	272	360	338	374	462	289	346	367	322	337	326	336	323	348	321	377
Y	17	19	17	14	b.d.l.	25	14	22	17	16	22	16	16	23	20	14
Zr	115	113	125	136	96	117	123	124	119	132	122	133	123	104	120	142
Nb	b.d.l.	5	b.d.l.	b.d.l.	b.d.l.	5	b.d.l.	5	b.d.l.	b.d.l.	6	b.d.l.	b.d.l.	4	5	b.d.l.
Sb	0.21	0.18	0.26	0.21	0.14	0.15	0.29	0.19	0.25	0.25	0.21	0.21	0.37	0.23	0.09	0.20
Cs	3.55	3.31	5.02	4.33	1.80	3.98	4.16	3.51	4.77	4.25	3.86	4.39	4.36	3.46	4.80	3.49
Ba	549	521	670	627	287	704	592	583	657	625	591	592	565	479	754	459
La	17.8	15.1	18.9	17.6	14.7	18.8	16.4	17.8	19.1	19.3	19.0	20.4	19.7	15.5	17.4	18.8
Ce	35.6	32.8	39.9	37.6	25.6	40.8	34.9	38.7	39.9	40.8	39.5	44.4	41.6	35.3	37.5	40.1
Nd	19.7	15.7	20.6	18.8	12.7	18.9	17.5	18.5	19.3	18.2	19.6	20.1	20.7	16.6	17.0	20.1
Sm	3.59	2.86	3.77	3.60	2.71	3.83	3.43	3.23	3.76	3.97	3.42	3.95	3.95	3.46	3.20	3.79
Eu	1.04	0.92	1.09	0.98	0.76	1.07	0.93	1.03	1.05	1.12	1.04	1.11	1.07	1.03	1.01	1.16
Gd	2.89	2.35	n.d.	n.d.	n.d.	3.28	n.d.	2.94	n.d.	2.92	2.67	3.21	2.92	3.00	2.06	2.80
Tb	0.46	0.37	0.47	0.44	0.30	0.65	0.41	0.52	0.47	0.53	0.54	0.51	0.52	0.51	0.51	0.45
Tm	0.28	0.21	<0.1	<0.1	<0.1	0.37	0.02	0.31	<0.1	0.27	0.24	0.27	0.28	0.29	0.24	0.25
Yb	2.17	1.23	1.54	1.41	1.44	2.06	1.36	1.42	1.6	1.60	1.54	1.86	1.63	1.56	1.43	1.57
Lu	0.30	0.18	0.26	0.23	0.22	0.29	0.22	0.20	0.26	0.24	0.23	0.28	0.24	0.24	0.21	0.23
Hf	2.60	2.84	3.02	3.07	1.99	2.82	2.99	2.9	3.36	3.21	3.06	3.40	3.01	2.86	2.81	3.20
Ta	0.34	0.28	0.41	0.37	0.22	0.41	0.43	0.27	0.31	0.36	0.31	0.39	0.43	0.33	0.30	0.37
Au (ppb)	<1.5	0.20	<1.3	1.10	<1.1	<1.1	<0.9	<1.0	<1.8	0.60	0.74	0.40	<1.9	1.30	0.79	<1.3
Th	2.74	2.49	3.30	3.02	2.10	3.26	3.11	2.51	3.26	3.18	3.04	3.43	3.58	3.09	2.85	2.89
U	0.86	0.52	1.36	1.01	0.77	1.52	1.24	0.95	1.26	1.14	1.03	1.36	1.38	1.02	0.92	1.16

[a]Samples analyzed for major and some trace elements at the Museum for Natural History, Humboldt University, Berlin. LB = lithic breccia; SB = suevitic breccia; MB = monomict breccia; G = granophyric-textured lithology, B = basement metasediments; b.d.l. = below detection limit; n.d. = not detected. LOI = loss on ignition. All major element concentrations in wt%, all trace element concentrations in ppm (unless stated otherwise).

Table 1. *Continued.* Major- (wt%) and trace-element (ppm, unless indicated otherwise) data for samples from the LB-07A borehole.

Sample no.	KR7-35	KR7-64[a]	KR7-6	KR7-65[a]	KR7-7a	KR7-7b	KR7-36a	KR7-36b	KR7-8	KR7-66[a]	KR7-9	KR7-50	KR7-37	KR7-10	KR7-67[a]	KR7-51
Depth (m)	359.33	359.96	360.65	362.99	363.2	363.2	364.45	364.45	370.34	370.39	377.46	378.20	379.09	380.21	382.94	383.14
Lithology	SB	SB	SB	SB	SB	SB	SB	SB	LB	LB	LB	SB	SB	SB	SB	SB
SiO_2	63.1	60.9	58.5	61.9	61.9	66.9	62.9	61.8	60.0	56.5	46.4	63.0	60.9	65.4	60.9	60.0
TiO_2	0.60	0.55	0.59	0.59	0.57	0.50	0.53	0.53	0.49	0.37	0.26	0.54	0.54	0.56	0.55	0.56
Al_2O_3	16.4	15.7	14.5	16.9	16.4	14.8	15.4	13.7	14.2	9.80	5.98	15.2	15.1	14.9	15.8	15.7
Fe_2O_3	5.90	6.21	6.21	6.38	6.08	6.24	5.58	5.39	5.87	6.91	7.23	6.11	5.99	5.96	6.91	6.62
MnO	0.07	0.06	0.05	0.05	0.06	0.06	0.06	0.05	0.06	0.08	0.14	0.05	0.06	0.05	0.05	0.05
MgO	2.83	3.79	3.53	2.75	2.32	2.17	2.15	2.69	4.06	9.78	15.0	2.27	4.00	3.08	4.51	3.84
CaO	2.36	2.70	2.10	1.84	1.90	0.95	1.95	2.36	1.09	4.61	6.84	1.47	1.97	1.03	1.61	1.09
Na_2O	2.54	2.66	2.39	2.59	2.60	3.28	2.59	3.06	3.78	0.94	0.03	2.43	2.28	3.20	2.81	3.10
K_2O	1.78	1.83	1.77	2.17	1.84	0.89	1.60	1.51	1.66	0.71	0.06	1.83	1.61	1.66	1.95	1.62
P_2O_5	0.09	0.09	0.08	0.11	0.09	0.09	0.09	0.09	0.11	0.06	0.05	0.06	0.09	0.10	0.09	0.17
LOI	4.88	5.20	10.4	4.10	5.22	2.72	6.93	7.24	6.31	9.70	17.2	6.99	6.41	3.66	4.8	5.85
SO_3		0.2		0.4						0.20					<0.1	
Total	100.6	99.9	100.6	99.8	99.0	98.6	99.8	98.4	97.7	99.7	99.1	100.0	99.0	99.6	100.0	98.6
Sc	15.3	15.4	14.6	17.5	12.6	15.6	13.9	14.7	13.9	15.8	18.6	15.7	13.1	13.5	15.8	16.2
V	126	113	136	130	98	125	118	123	126	96	84	134	122	133	120	126
Cr	186	152	194	104	123	160	160	158	347	882	2023	236	279	147	218	196
Co	17.0	21.0	16.0	18.8	13.0	17.6	15.1	16.0	18.9	41.5	77.0	17.7	19.0	16.0	22.2	20.1
Ni	63	84	88	50	34	53	49	53	134	714	1418	90	118	44	130	86
Cu	30	46	19	52	16	29	23	26	25	71	103	38	22	33	43	24
Zn	73	77	77	86	79	75	63	70	65	65	52	79	74	65	77	80
As	6.83	16.5	14.0	8.47	0.87	10.6	4.69	4.99	72.3	401	728	16.5	12.7	3.02	34.1	22.9
Se	0.16	<2.6	0.09	0.67	0.10	0.22	0.17	0.18	0.20	<2.6	0.95	0.19	0.17	0.18	<2.5	0.24
Br	<1.1	0.5	<0.4	0.5	<0.5	<0.4	<0.5	<0.5	<0.4	0.4	<0.3	<1.2	<1.1	<0.4	0.6	<1.2
Rb	68	69	84	84	35	78	70	74	71	31	2	66	65	71	70	79
Sr	332	320	305	359	378	339	317	343	348	300	309	282	351	295	356	336
Y	22	13	25	16	20	23	22	23	21	b.d.l.	13	21	21	23	12	23
Zr	116	113	114	113	106	122	127	122	116	59	45	122	115	122	123	121
Nb	5	b.d.l.	6	b.d.l.	4	6	5	6	5	b.d.l.	3	6	5	6	b.d.l.	6
Sb	0.14	0.24	0.12	0.20	0.18	0.25	0.22	0.25	0.55	2.55	0.60	0.13	0.28	0.12	0.37	0.40
Cs	3.49	3.42	3.52	4.21	1.92	3.91	3.42	3.67	3.69	1.66	3.02	4.18	3.63	3.47	3.99	4.11
Ba	525	476	518	569	262	534	467	504	525	484	34.0	536	468	648	542	636
La	17.2	16.3	17.5	18.3	14.7	19.6	21.1	21.2	15.3	10.3	5.00	18.6	17.4	17.0	19.2	17.7
Ce	40.7	35.1	34.5	40.2	32.9	43.0	41.3	42.2	33.4	22.6	11.0	42.7	36.9	36.8	40.2	41.2
Nd	20.2	17.4	17.7	19.7	16.6	20.4	21.1	21.6	16.7	10.2	5.74	21.3	19.2	18.0	19.5	21.3
Sm	3.35	3.17	3.34	3.60	2.97	3.75	3.69	3.87	2.92	2.13	1.15	3.82	3.47	3.02	3.61	3.86
Eu	1.02	1.02	1.01	1.10	0.96	1.13	1.12	1.18	0.88	0.65	0.42	1.15	1.10	0.96	1.05	1.10
Gd	3.02	3.07	2.27	2.94	2.45	3.24	4.07	4.32	2.68	1.96	1.04	3.38	2.70	2.54	3.06	3.35
Tb	0.49	0.42	0.52	0.47	0.43	0.58	0.50	0.59	0.53	0.32	0.18	0.54	0.52	0.46	0.46	0.52
Tm	0.27	0.22	0.31	0.21	0.22	0.25	0.25	0.34	0.31	0.20	0.11	0.30	0.29	0.22	0.20	0.28
Yb	1.38	1.43	1.49	1.70	1.49	1.66	1.60	1.87	1.66	1.22	0.46	1.88	1.41	1.41	1.57	1.63
Lu	0.23	0.22	0.21	0.27	0.21	0.24	0.23	0.28	0.24	0.15	0.08	0.28	0.23	0.20	0.24	0.24
Hf	2.58	2.87	2.58	3.02	2.75	3.13	3.28	3.21	2.57	1.63	0.90	3.39	3.72	2.91	3.15	3.55
Ta	0.27	0.30	0.27	0.37	0.27	0.31	0.34	0.35	0.29	0.19	0.25	0.36	0.34	0.27	0.35	0.39
Au (ppb)	0.6	<1.3	<1.0	<1.2	<1.6	<1.4	<1.3	<1.6	1.4	<1.2	0.5	1.4	<1.3	<1.4	0.8	1.4
Th	2.99	2.63	2.70	3.16	2.28	3.32	3.50	3.69	2.66	1.60	0.51	3.51	3.01	2.77	3.31	3.30
U	0.98	0.88	1.00	1.14	0.16	1.25	1.33	1.24	0.97	0.77	0.33	0.62	0.82	0.80	0.87	1.22

[a]Samples analyzed for major and some trace elements at the Museum for Natural History, Humboldt University, Berlin. LB = lithic breccia; SB = suevitic breccia; MB = monomict breccia; G = granophyric-textured lithology, B = basement metasediments; b.d.l. = below detection limit; n.d. = not detected. LOI = loss on ignition. All major element concentrations in wt%, all trace element concentrations in ppm (unless stated otherwise).

Table 1. *Continued.* Major- (wt%) and trace-element (ppm, unless indicated otherwise) data for samples from the LB-07A borehole.

Sample no.	KR7-11a	KR711b	KR7-43a	KR7-43b	KR7-43c	KR7-38	KR7-68[a]	KR7-39	KR7-12	KR7-52a	KR7-52b	KR7-52c	KR7-13	KR7-69[a]	KR7-14	KR7-70[a]
Depth (m)	383.74	383.74	384.84	384.84	384.84	387.59	390.23	390.85	391.85	392.00	392.00	392.00	393.78	395.14	398.44	398.58
Lithology	SB	SB	SB	SB	SB	SB	SB	SB	LB	LB	LB	LB	LB	SB	SB	SB
SiO_2	59.9	53.8	63.2	56.7	59.2	61.4	63.3	62.2	61.2	66.2	58.7	63.8	64.5	63.9	64.0	70.0
TiO_2	0.65	0.29	0.50	0.38	0.59	0.61	0.66	0.67	0.55	0.41	0.58	0.40	0.56	0.55	0.47	0.39
Al_2O_3	15.3	5.02	13.3	13.2	13.7	17.0	16.2	17.4	14.9	14.5	14.9	16.2	14.2	1.54	14.6	12.6
Fe_2O_3	7.53	5.50	4.73	4.88	5.41	5.94	6.72	6.78	6.12	5.43	6.79	4.50	5.58	5.92	5.46	4.11
MnO	0.05	0.12	0.07	0.02	0.07	0.05	0.04	0.06	0.04	0.03	0.06	0.03	0.04	0.05	0.05	0.05
MgO	4.84	12.7	1.85	3.79	3.44	2.31	2.32	2.86	2.93	1.99	4.31	2.34	2.90	2.63	2.24	1.62
CaO	1.21	6.40	2.45	10.1	3.57	1.61	1.11	1.43	1.90	1.65	1.76	1.79	1.62	1.97	1.88	2.53
Na_2O	2.40	0.11	2.33	1.75	3.71	2.41	2.33	2.00	2.67	2.73	3.15	2.77	2.85	2.73	2.56	3.57
K_2O	2.05	0.00	1.75	1.32	1.49	2.00	2.26	2.44	1.87	1.17	1.79	1.52	1.68	2.10	1.58	1.20
P_2O_5	0.12	0.07	0.08	0.18	0.13	0.11	0.06	0.09	0.10	0.14	0.09	0.10	0.10	0.08	0.09	0.43
LOI	5.87	15.1	8.39	7.85	8.53	5.94	4.2	4.97	7.90	4.34	7.68	5.20	6.72	4.30	5.79	3.00
SO_3							0.4							0.2		<0.1
Total	99.9	99.1	98.6	101.2	99.9	99.5	99.1	100.8	100.2	98.9	99.7	98.7	100.7	99.8	98.7	99.5
Sc	17.8	17.2	12.1	17.2	12.3	16.3	16.3	18.1	15.2	11.0	16.6	11.4	13.3	14.6	12.1	9.13
V	135	89	98	155	101	135	122	149	150	96	140	114	145	114	112	74
Cr	197	1765	127	389	114	177	111	179	342	107	336	125	161	112	172	80
Co	22.8	39.7	13.5	20.0	16.0	16.8	24.2	21.0	18.0	10.2	21.1	12.6	15.4	19.1	22.4	9.57
Ni	101	605	31	177	33	68	61	59	52	24	125	31	78	91	466	27
Cu	35	22	31	34	13	29	48	32	27	46	46	31	28	48	76	45
Zn	79	45	57	76	58	77	86	87	73	56	83	51	68	78	60	56
As	22.5	159	1.09	21.7	2.38	5.01	2.11	6.30	6.57	0.64	12.4	0.26	12.9	23.0	33.4	7.16
Se	0.26	0.14	0.16	0.15	0.15	0.18	<2.8	0.27	0.23	0.20	0.20	0.20	0.19	<2.6	0.22	<2.2
Br	<0.4	<0.2	0.2	<0.2	<0.5	<0.1	0.6	<1.2	<0.4	<0.5	<1.1	<0.5	<0.4	0.6	<0.4	0.6
Rb	91	5.0	77	70	67	86	86	104	86	58	78	75	76	80	62	42
Sr	239	221	296	289	393	326	331	255	280	351	297	258	302	309	340	376
Y	25	15	24	22	21	23	22	26	23	18	22	20	22	16	21	13
Zr	129	56	120	122	124	130	150	140	120	147	117	114	130	143	114	133
Nb	6	3	6	5	5	6	b.d.l.	6	6	5	5	5	6	b.d.l.	4	b.d.l.
Sb	0.15	0.74	0.28	0.24	0.10	0.20	0.73	0.19	0.07	0.07	0.20	0.13	0.12	0.27	0.25	0.24
Cs	4.37	0.41	4.16	3.72	3.64	4.14	3.78	5.40	4.33	3.44	4.03	3.99	3.85	4.42	3.02	1.96
Ba	537	27	477	491	387	587	523	585	597	349	504	521	553	507	527	505
La	21.0	6.62	16.8	17.5	14.2	20.7	19.7	23.9	18.8	19.5	17.5	15.4	18.6	21.1	16.4	20.1
Ce	44.3	14.4	35.0	37.4	29.9	41.7	44.6	51.0	40.8	41.2	39.7	31.9	37.5	45.3	32.0	43.9
Nd	21.8	7.28	17.7	18.7	14.8	21.2	21.6	25.3	20.3	20.3	19.8	16.1	18.8	22.0	16.2	22.8
Sm	3.91	1.49	3.37	3.22	3.02	3.71	4.14	4.27	3.45	3.26	3.35	2.91	3.46	3.90	2.90	4.08
Eu	1.06	0.40	1.02	1.02	0.74	1.16	1.16	1.29	1.05	1.11	1.03	0.87	0.98	1.16	0.91	1.14
Gd	3.89	1.20	3.18	2.17	3.75	4.11	3.38	4.74	3.30	2.24	2.80	3.35	2.79	3.51	3.59	3.06
Tb	0.62	0.30	0.51	0.44	0.42	0.64	0.57	0.56	0.64	0.40	0.48	0.42	0.53	0.50	0.43	0.45
Tm	0.28	0.17	0.30	0.22	0.22	0.37	0.31	0.24	0.33	0.22	0.27	0.25	0.30	0.26	0.22	0.24
Yb	1.91	0.58	1.66	1.62	1.12	2.25	2.17	1.92	1.56	1.23	1.49	1.45	1.44	1.75	1.37	1.68
Lu	0.28	0.09	0.23	0.24	0.19	0.31	0.33	0.31	0.24	0.17	0.24	0.21	0.20	0.27	0.21	0.26
Hf	3.31	1.04	3.03	3.07	2.89	3.18	3.61	3.82	2.93	3.81	3.02	3.00	2.81	3.33	2.75	2.80
Ta	0.42	0.11	0.34	0.31	0.25	0.35	0.46	0.43	0.32	0.28	0.33	0.39	0.36	0.40	0.26	0.29
Au (ppb)	0.6	<0.8	0.6	0.7	0.4	0.6	2.5	0.7	0.6	<1.5	0.5	<1.4	<1.0	1.2	1.5	<1.4
Th	3.76	0.82	3.16	2.99	2.49	3.33	4.09	4.32	3.17	4.20	3.28	2.95	3.45	3.49	2.64	2.87
U	1.58	0.36	1.15	1.34	1.06	0.83	1.31	1.28	1.14	0.94	0.95	0.88	1.31	1.17	0.90	3.79

[a]Samples analyzed for major and some trace elements at the Museum for Natural History, Humboldt University, Berlin. LB = lithic breccia; SB = suevitic breccia; MB = monomict breccia; G = granophyric-textured lithology, B = basement metasediments; b.d.l. = below detection limit; n.d. = not detected. LOI = loss on ignition. All major element concentrations in wt%, all trace element concentrations in ppm (unless stated otherwise).

Table 1. *Continued.* Major- (wt%) and trace-element (ppm, unless indicated otherwise) data for samples from the LB-07A borehole.

Sample no.	KR7-40	KR7-53	KR7-15	KR7-16	KR7-17	KR7-44	KR7-20	KR7-41	KR7-41a	KR7-18	KR7-42	KR7-21	KR7-71[a]	KR7-72[a]	KR7-22	KR7-73[a]
Depth (m)	400.06	400.58	402.73	404.26	405.57	407.77	408.72	408.72	408.72	411.34	412.17	413.13	415.67	416.07	420.86	421.56
Lithology	SB	SB	SB	SB	SB	SB	SB	SB	SB	SB	SB	SB	MB	MB	MB	MB
SiO_2	65.3	59.9	62.5	58.6	64.2	63.7	61.3	64.1	60.9	61.6	57.1	54.9	65.1	72.7	56.0	69.6
TiO_2	0.49	0.65	0.59	0.56	0.53	0.58	0.55	0.54	0.51	0.51	0.66	0.50	0.44	0.36	0.51	0.44
Al_2O_3	14.4	16.0	15.7	14.5	14.8	14.7	15.1	14.8	14.7	16.3	16.9	12.4	15.6	10.9	12.7	13.9
Fe_2O_3	5.22	6.45	6.13	5.78	5.53	6.00	5.73	5.54	5.39	5.29	6.65	6.50	2.96	3.74	6.46	4.77
MnO	0.06	0.05	0.05	0.06	0.06	0.05	0.05	0.06	0.06	0.06	0.06	0.10	0.06	0.05	0.12	0.04
MgO	1.97	1.87	2.87	2.62	2.08	1.56	2.86	2.73	1.99	1.73	3.46	6.40	1.32	1.41	4.44	1.75
CaO	2.20	1.97	1.61	1.97	2.05	2.62	2.46	2.28	2.22	2.06	2.06	5.19	3.94	2.58	6.48	1.45
Na_2O	2.61	2.24	2.96	5.38	2.87	2.58	2.69	1.32	3.16	2.74	3.08	1.66	2.30	2.38	1.88	2.72
K_2O	1.60	2.52	2.01	1.80	1.96	1.98	1.87	1.72	1.75	1.98	1.93	1.27	2.87	1.13	1.13	1.60
P_2O_5	0.37	0.04	0.14	0.10	0.10	0.05	0.14	0.13	0.11	0.11	0.12	0.12	0.09	0.05	0.13	0.08
LOI	4.42	8.80	6.11	7.76	5.27	4.82	6.35	5.81	9.02	6.31	8.17	9.53	4.9	4.0	8.99	2.9
SO_3													<0.1	<0.1		<0.1
Total	98.7	100.1	100.7	99.2	99.5	98.6	99.1	99.0	99.7	98.7	100.2	98.6	99.6	99.0	98.8	99.3
Sc	12.6	17.5	15.7	14.8	14.3	15.7	14.5	8.89	12.8	12.9	17.6	10.9	7.25	7.82	17.5	10.2
V	102	142	129	151	116	122	132	102	93	111	145	94	54	72	147	89
Cr	156	136	183	149	128	145	151	102	110	111	148	457	49	69	459	75
Co	14.0	19.0	15.0	17.0	16.0	16.6	15.4	10.0	13.0	15.0	16.1	29.3	5.98	10.1	20.0	10.5
Ni	74	53	46	53	47	49	50	24	46	36	51	292	b.d.l.	b.d.l.	110	17
Cu	29	40	32	28	30	31	26	28	28	19	34	b.d.l.	b.d.l.	b.d.l.	b.d.l.	b.d.l.
Zn	60	82	72	70	66	71	68	45	69	64	86	79	47	56	83	66
As	7.77	4.78	15.7	11.0	9.56	5.03	4.56	1.52	4.50	7.75	4.42	55.1	0.13	<0.70	8.32	<0.88
Se	0.12	0.20	0.18	0.15	0.19	0.15	0.13	0.15	0.14	0.10	0.18	0.11	<1.9	<1.9	0.03	<2.2
Br	<1.2	<0.4	<0.4	<0.4	<0.4	<0.5	<0.5	<1.3	<1.2	<0.4	<1.1	0.12	0.3	0.5	<0.4	0.6
Rb	60	91	80	75	72	80	72	49	66	69	82	53	103	45	54	63
Sr	329	361	383	374	374	375	351	431	372	411	395	373	378	272	359	337
Y	27	26	23	24	23	22	22	21	116	23	24	18	13	<10	23	b.d.l.
Zr	126	125	123	122	116	122	126	125	116	137	135	94	109	129	89	128
Nb	5	6	5	6	5	6	5	6	4	5	6	4	b.d.l.	b.d.l.	4	b.d.l.
Sb	0.23	0.27	0.29	0.22	0.19	0.27	0.24	<0.2	0.33	0.09	0.12	0.10	0.04	0.01	0.21	0.10
Cs	3.30	4.65	4.44	3.65	4.13	4.26	3.78	3.43	4.17	4.02	5.19	3.50	5.14	1.98	2.56	2.69
Ba	512	760	654	565	562	552	645	440	537	649	671	469	824	328	346	410
La	20.8	21.2	17.7	17.1	18.0	19.5	18.9	10.6	15.6	19.8	19.5	11.8	13.5	18.4	16.2	14.6
Ce	47.2	42.4	37.8	38.0	38.8	41.0	37.9	24.3	34.4	40.7	44.6	25.5	28.9	37.6	34.2	31.2
Nd	24.4	22.1	19.4	17.4	19.9	20.3	19.1	11.9	18.2	21.1	21.7	13.7	14.8	16.9	18.4	15.1
Sm	4.26	4.01	3.41	3.21	3.44	3.57	3.44	1.86	3.08	3.35	3.71	2.59	2.85	2.97	3.43	2.57
Eu	1.39	1.28	1.02	1.00	1.04	1.14	1.08	0.67	0.86	0.99	1.14	0.84	0.78	0.88	1.06	0.76
Gd	3.12	4.21	3.95	2.79	3.95	4.01	3.94	2.48	2.35	2.89	3.16	1.89	1.93	2.14	3.41	1.90
Tb	0.55	0.68	0.52	0.53	0.52	0.52	0.53	0.29	0.54	0.52	0.50	0.34	0.31	0.35	0.60	0.30
Tm	0.30	0.36	0.26	0.31	0.31	0.26	0.30	0.17	0.36	0.30	0.29	0.16	0.18	0.16	0.27	0.17
Yb	1.85	2.21	1.70	1.42	1.66	1.59	1.96	1.15	1.40	1.69	1.74	0.98	0.97	1.02	1.56	1.05
Lu	0.28	0.31	0.26	0.22	0.23	0.25	0.27	0.16	0.22	0.25	0.28	0.15	0.14	0.16	0.23	0.16
Hf	3.54	3.21	3.15	2.84	2.94	3.21	3.27	3.08	2.71	3.29	3.35	2.38	2.68	2.85	2.18	2.67
Ta	0.32	0.38	0.38	0.34	0.34	0.35	0.31	0.29	0.35	0.32	0.39	0.22	0.23	0.27	0.22	0.25
Au (ppb)	<1.4	0.19	0.80	1.26	0.68	1.20	0.82	<1.4	0.60	<1.4	1.95	<1.3	<1.5	<1.5	0.38	<1.2
Th	3.39	3.50	3.17	2.88	2.99	3.31	3.05	3.18	2.97	3.21	3.97	1.87	2.29	3.59	2.36	2.41
U	1.49	1.20	1.35	0.89	0.81	0.90	0.95	0.50	1.17	0.80	1.40	0.69	<0.6	0.95	0.84	0.72

[a]Samples analyzed for major and some trace elements at the Museum for Natural History, Humboldt University, Berlin. LB = lithic breccia; SB = suevitic breccia; MB = monomict breccia; G = granophyric-textured lithology, B = basement metasediments; b.d.l. = below detection limit; n.d. = not detected. LOI = loss on ignition. All major element concentrations in wt%, all trace element concentrations in ppm (unless stated otherwise).

Table 1. *Continued.* Major- (wt%) and trace-element (ppm, unless indicated otherwise) data for samples from the LB-07A borehole.

Sample no.	KR7-74[a]	KR7-23	KR7-75[a]	KR7-24	KR7-25	KR7-76[a]	KR7-77[a]	KR7-45	KR7-78[a]	KR7-26	KR7-79[a]	KR7-27	KR7-28	KR7-80[a]	KR7-29	KR7-81[a]
Depth (m)	430.03	430.13	430.28	439.01	439.61	441.60	445.13	445.22	450.37	454.35	454.52	468.28	470.55	471.88	475.76	483.00
Lithology	SB	SB	MB	MB	MB	MB	SB	SB	MB	MB	MB	MB	MB	B	B	SB
SiO_2	64.9	61.2	69.5	58.3	57.8	61.6	64.3	63.2	67.0	77.0	68.3	67.8	65.4	52.7	64.5	62.7
TiO_2	0.56	0.57	0.41	0.67	0.62	0.67	0.56	0.57	0.49	0.34	0.45	0.48	0.54	0.38	0.60	0.64
Al_2O_3	16.3	14.3	12.9	19.7	19.0	18.3	14.8	15.6	15.2	10.3	15.5	14.2	14.4	12.1	16.3	15.9
Fe_2O_3	5.70	6.33	3.88	7.31	7.44	6.81	5.88	6.04	4.87	3.92	4.39	4.99	5.49	5.34	6.79	6.73
MnO	0.04	0.07	0.06	0.05	0.05	0.04	0.06	0.04	0.04	0.04	0.03	0.06	0.06	0.11	0.05	0.04
MgO	2.28	4.05	1.44	2.53	2.68	2.50	2.16	1.90	1.78	1.93	1.51	1.63	2.70	6.60	2.37	2.44
CaO	1.77	2.89	3.14	1.16	2.10	0.82	2.50	1.96	1.68	1.41	1.14	2.50	1.50	6.50	0.60	1.16
Na_2O	3.06	2.57	3.08	2.38	2.04	2.56	3.32	2.68	4.45	1.29	4.37	2.00	3.29	1.50	2.50	2.57
K_2O	1.89	1.58	1.50	2.46	2.46	2.67	1.49	1.62	1.16	0.57	1.48	1.77	1.52	1.62	2.20	2.34
P_2O_5	0.08	0.13	0.06	0.08	0.08	0.07	0.12	0.05	0.09	0.08	0.07	0.14	0.11	0.09	0.10	0.09
LOI	3.4	6.13	4.00	4.09	4.16	3.50	4.30	6.23	2.60	2.14	2.20	4.03	3.33	12.3	4.11	4.70
SO_3	<0.1		<0.1			<0.1	0.1		0.1		<0.1			<0.1		0.2
Total	100.0	99.9	100.0	98.7	98.4	99.5	99.6	99.9	99.5	99.0	99.4	99.6	98.3	99.2	100.2	99.5
Sc	12.5	15.3	9.50	20.8	21.7	18.0	12.9	14.8	10.5	6.69	9.74	0.19	1.81	10.0	0.07	15.6
V	110	133	84	187	163	133	105	129	94	136	88	117	125	74	140	133
Cr	91	148	73	170	152	96	89	140	87	158	77	99	143	261	168	109
Co	13.1	15.1	9.09	19.7	19.0	19.1	16.6	16.0	11.6	15.0	9.61	12.4	15.0	21.3	19.9	20.1
Ni	33	54	16	47	48	53	28	47	25	18	b.d.l.	27	43	224	39	45
Cu	49	25	38	44	42	59	60	28	49	19	31	32	30	b.d.l.	29	39
Zn	77	78	54	89	96	90	76	75	66	39	51	58	64	83	80	87
As	3.50	3.79	<0.9	0.42	0.84	<0.9	3.81	3.37	<11	<0.4	<1.4	0.19	1.81	65.0	0.07	2.30
Se	<2.6	0.16	<2.0	0.20	0.19	<2.7	<2.5	0.15	<2.2	0.09	<2.1	0.14	0.17	<1.8	0.24	<2.3
Br	0.4	<1.0	0.4	<0.5	<0.5	0.3	0.7	<1.2	0.4	<0.5	0.3	<0.5	<0.5	0.4	<0.5	0.6
Rb	72	70	60	101	108	104	58	70	47	29	61	77	70	72	94	93
Sr	342	382	334	364	316	306	399	384	379	251	398	280	349	267	221	247
Y	13	24	b.d.l.	23	27	19	14	26	b.d.l.	18	b.d.l.	23	21	b.d.l.	27	23
Zr	128	122	117	125	120	119	180	122	162	100	148	116	139	70	139	164
Nb	b.d.l.	5	b.d.l.	6	6	b.d.l.	b.d.l.	6	b.d.l.	4	b.d.l.	4	5	b.d.l.	6	b.d.l.
Sb	0.14	0.13	0.09	0.14	0.09	0.06	0.22	<0.2	<0.2	0.12	0.16	0.14	0.11	0.29	0.11	0.16
Cs	3.71	3.92	2.72	4.64	4.71	4.87	3.76	4.14	2.23	1.38	2.78	4.04	3.85	4.05	5.34	5.84
Ba	471	556	394	739	737	701	485	539	341	214	402	582	531	282	509	500
La	17.1	19.9	16.8	18.6	20.7	11.5	24.1	18.2	16.2	18.8	15.5	18.6	20.8	8.82	20.6	24.3
Ce	34.3	42.8	34.4	41.3	42.8	24.9	50.8	42.1	34.3	36.2	32.9	39.3	40.6	19.1	43.9	50.6
Nd	16.1	22.1	15.8	20.3	20.8	13.4	21.7	21.3	15.3	16.2	14.6	19.5	20.7	11.0	21.6	26.2
Sm	2.97	4.06	2.63	3.38	3.96	2.47	4.36	3.83	2.84	2.54	2.78	3.36	3.64	1.98	4.22	4.61
Eu	1.00	1.21	0.87	1.09	1.14	0.78	1.32	1.14	0.95	0.78	0.82	1.10	1.08	0.61	1.30	1.27
Gd	3.07	3.56	2.20	4.01	4.61	2.35	3.35	2.90	2.09	2.64	2.05	2.93	4.21	n.d.	3.54	n.d.
Tb	0.42	0.55	0.32	0.57	0.61	0.35	0.59	0.51	0.36	0.30	0.34	0.46	0.54	0.26	0.71	0.54
Tm	0.17	0.27	0.16	0.31	0.31	0.17	0.28	0.30	0.19	0.17	0.16	0.28	0.25	<0.1	0.40	0.06
Yb	1.14	1.62	0.87	2.04	2.15	1.21	2.11	1.57	1.41	0.98	0.93	1.35	1.62	0.70	2.22	1.99
Lu	0.16	0.26	0.14	0.29	0.33	0.20	0.31	0.24	0.21	0.14	0.15	0.23	0.23	0.11	0.33	0.32
Hf	2.81	3.14	2.66	3.28	2.92	3.02	3.88	2.89	3.74	2.42	3.00	2.92	4.06	1.92	3.54	3.71
Ta	0.35	0.35	0.27	0.37	0.34	0.43	0.38	0.35	0.27	0.23	0.30	0.36	0.37	0.15	0.48	0.51
Au (ppb)	<1.7	<1.1	<1.0	1.2	0.9	0.4	<1.6	1.4	<1.7	<1.4	<1.4	<1.4	<1.3	<0.9	1.9	<1.2
Th	2.64	3.06	2.31	3.75	3.40	3.22	3.92	3.30	2.56	2.44	2.31	2.75	3.36	1.38	4.12	4.35
U	0.86	1.12	0.69	1.23	1.32	1.04	1.45	1.11	0.90	0.49	0.80	1.05	1.16	0.56	1.06	1.82

[a]Samples analyzed for major and some trace elements at the Museum for Natural History, Humboldt University, Berlin. LB = lithic breccia; SB = suevitic breccia; MB = monomict breccia; G = granophyric-textured lithology, B = basement metasediments; b.d.l. = below detection limit; n.d. = not detected. LOI = loss on ignition. All major element concentrations in wt%, all trace element concentrations in ppm (unless stated otherwise).

Table 1. *Continued.* Major- (wt%) and trace-element (ppm, unless indicated otherwise) data for samples from the LB-07A borehole.

Sample no.	KR7-82[a]	KR7-29A	KR7-30	KR7-31	KR7-83[a]	KR7-32	KR7-46	KR7-47	KR7-84[a]	KR7-48	KR7-49	KR7-85[a]	KR7-33
Depth (m)	487.12	487.36	491.01	512.15	513.90	514.77	530.63	530.79	538.29	538.89	538.99	539.66	542.70
Lithology	G	B	B	B	SB	B	B	B	B	B	B	B	B
SiO_2	51.2	49.7	63.3	62.2	79.1	54.1	60.2	68.8	73.3	68.5	58.1	58.1	60.8
TiO_2	0.51	0.46	0.70	0.54	0.51	0.60	0.57	0.57	0.43	0.59	0.48	0.48	0.72
Al_2O_3	12.1	10.4	17.8	15.2	6.80	12.8	18.6	13.7	12.3	14.3	13.9	14.2	18.6
Fe_2O_3	7.20	6.87	7.01	4.85	3.21	5.54	3.35	5.89	4.37	5.64	5.01	4.95	7.06
MnO	0.12	0.11	0.05	0.05	0.03	0.07	0.10	0.03	0.03	0.05	0.09	0.07	0.05
MgO	6.82	9.28	2.44	2.67	2.08	3.63	1.03	1.40	1.51	1.23	3.64	3.86	2.35
CaO	6.16	6.89	0.43	2.78	2.13	8.49	3.06	0.86	0.82	0.55	4.88	4.59	0.39
Na_2O	1.49	0.36	2.77	2.84	0.48	3.81	1.09	2.35	2.79	2.95	3.03	3.57	2.07
K_2O	1.22	0.79	2.23	1.94	1.17	0.83	5.20	1.89	1.37	1.70	1.44	1.47	2.62
P_2O_5	0.15	0.14	0.09	0.13	0.02	0.22	0.09	0.03	0.06	0.10	0.10	0.10	0.09
LOI	12.3	13.9	3.93	5.63	4.10	8.73	6.92	3.88	2.7	3.21	8.92	8.1	3.98
SO_3	<0.1				<0.1				<0.1			<0.1	
Total	99.3	98.9	100.8	98.8	99.6	98.9	100.3	99.4	99.7	98.8	99.5	99.5	98.7
Sc	15.6	17.8	17.9	12.8	7.10	12.6	16.4	14.7	8.50	13.5	12.5	12.5	20.2
V	103	117	148	120	78	116	90	130	75	121	91	82	168
Cr	405	785	159	106	85	219	31.4	145	151	161	258	140	178
Co	33.2	31.7	18.7	14.5	10.7	23.3	3.50	16.3	13.7	15.0	13.0	14.2	20.4
Ni	259	316	42	74	38	151	14	37	22	42	90	74	52
Cu	b.d.l.	b.d.l.	35	b.d.l.	b.d.l.	b.d.l.	13	24	b.d.l.	23	b.d.l.	b.d.l.	34
Zn	96	82	96	75	54	73	42	97	66	74	69	68	91
As	125	51.5	<0.8	35.3	22.3	39.3	<0.5	<0.7	1.61	4.05	16.7	21.7	0.46
Se	<3.2	0.20	0.28	0.20	<1.5	0.12	0.51	0.21	<1.7	0.28	0.01	<1.9	0.29
Br	0.5	<1.0	<1.3	<1.2	0.3	<0.6	<0.5	<1.2	0.4	<1.2	<1.2	0.4	<1.3
Rb	53	34	97	76	61	43	210	86	61	76	69	66	127
Sr	337	217	199	492	158	575	279	165	162	190	287	303	222
Y	b.d.l.	18	25	21	b.d.l.	20	75	25	11	28	19	b.d.l.	31
Zr	81	77	144	102	34	94	580	135	252	158	101	104	166
Nb	b.d.l.	3	8	7	b.d.l.	8	13	7	b.d.l.	7	3	b.d.l.	9
Sb	<0.1	0.17	0.12	0.09	0.16	<0.2	0.29	0.21	<0.1	<0.2	0.17	0.15	0.19
Cs	2.51	1.54	5.11	4.28	2.84	2.12	10.9	4.56	3.41	3.98	3.32	3.57	5.40
Ba	235	88	526	548	323	210	1071	454	319	410	394	366	598
La	18.0	16.0	25.5	20.5	7.96	19.5	101	22.1	21.4	23.0	11.4	13.2	27.2
Ce	40.0	32.2	53.6	42.2	17.3	40.4	210	46.4	45.0	51.5	27.2	27.2	53.7
Nd	24.0	16.0	22.5	20.1	8.64	20.1	110	22.5	21.2	25.8	13.4	13.7	27.2
Sm	4.34	3.53	4.33	3.71	1.52	3.28	19.7	3.72	3.91	4.35	2.35	2.90	5.00
Eu	1.18	1.01	1.20	1.12	0.44	1.09	4.32	1.09	0.98	1.25	0.77	0.79	1.36
Gd	n.d.	2.63	3.10	2.89	n.d.	3.38	10.7	3.51	n.d.	4.13	2.04	n.d.	2.65
Tb	0.38	0.40	0.54	0.45	0.17	0.39	2.52	0.54	0.45	0.65	0.34	0.35	0.67
Tm	<0.1	0.20	0.31	0.18	<0.1	0.21	1.32	0.32	0.04	0.30	0.18	<0.1	0.37
Yb	1.24	1.04	2.07	0.87	0.48	1.21	6.07	1.82	1.50	2.03	0.95	1.08	2.36
Lu	0.18	0.14	0.31	0.15	0.08	0.16	0.94	0.29	0.23	0.30	0.15	0.17	0.35
Hf	2.14	1.83	3.58	2.78	1.04	2.25	14.5	3.62	5.33	4.02	2.39	2.62	4.28
Ta	0.19	0.16	0.50	0.24	0.36	0.36	1.21	0.46	0.36	0.55	0.21	0.32	0.53
Au (ppb)	<1.0	<1.1	0.4	<1.3	<0.6	<0.4	1.1	0.9	<1.2	0.4	<1.5	<1.1	1.52
Th	2.31	1.77	4.51	2.89	1.20	2.50	8.06	4.07	4.95	4.44	1.94	2.19	5.04
U	0.91	0.54	1.40	1.26	0.90	1.05	4.69	1.51	1.49	1.31	0.61	1.26	1.63

[a]Samples analyzed for major and some trace elements at the Museum for Natural History, Humboldt University, Berlin. LB = lithic breccia; SB = suevitic breccia; MB = monomict breccia; G = granophyric-textured lithology, B = basement metasediments; b.d.l. = below detection limit; n.d. = not detected. LOI = loss on ignition. All major element concentrations in wt%, all trace element concentrations in ppm (unless stated otherwise).

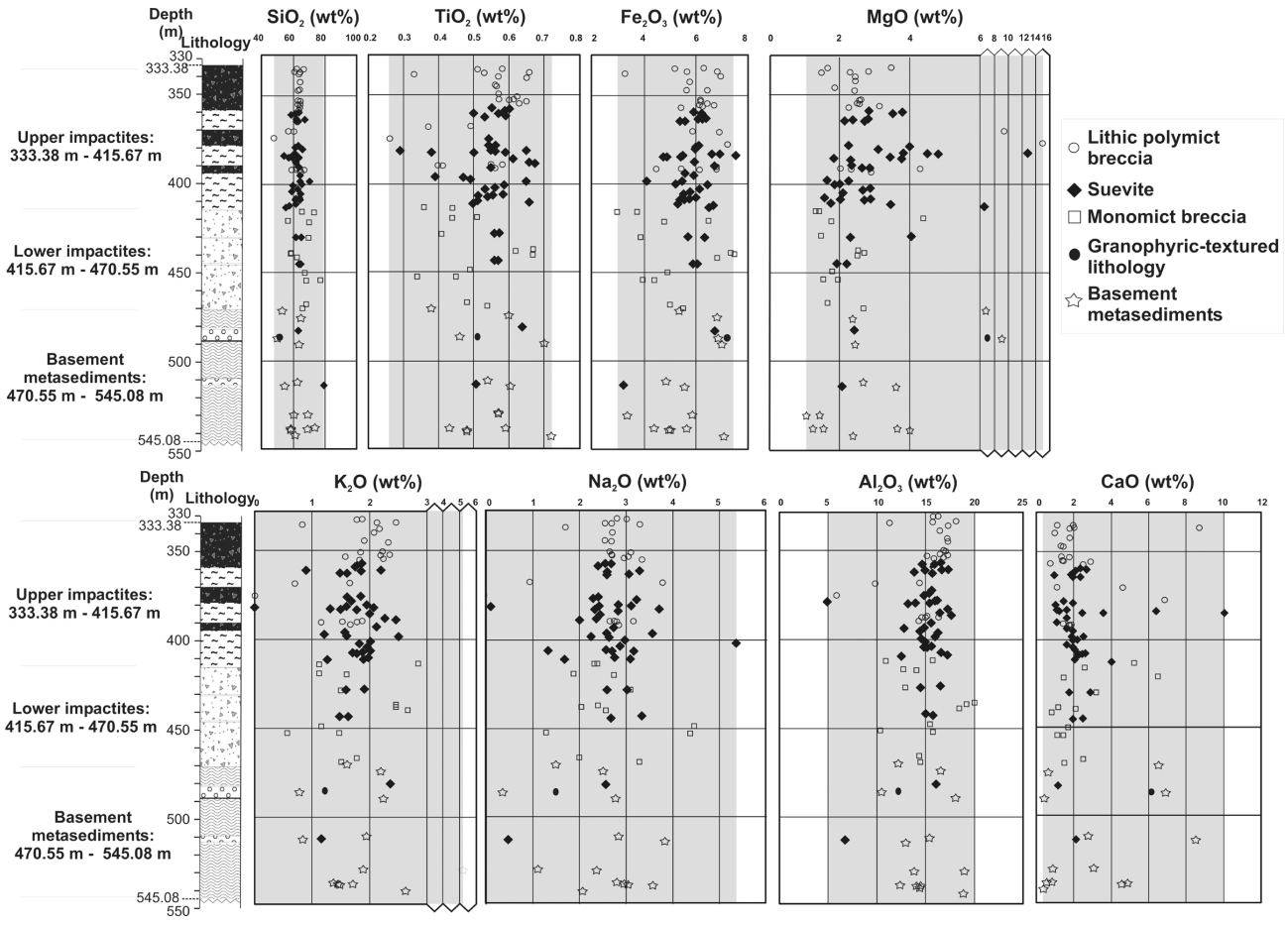

Fig. 1. Profiles of the major elements SiO_2, TiO_2, Fe_2O_3, MgO, K_2O, Na_2O, Al_2O_3, and CaO abundances versus depth for the LB-07A drill core.

Comparison of Upper and Lower Suevite Occurrences

In general, all suevite samples show similar geochemical signatures (Fig. 1). The lowermost suevite intercalation in the basement metasediments (at a depth of 513.90 m) has comparatively higher SiO_2 and lower Al_2O_3, Fe_2O_3, Na_2O, and K_2O contents than the average (Fig. 1; Table 1) suevite values. The major element compositions of the lower impactite (at depths of 430.03 m and 445.13 m) and upper basement (at a depth of 483.00 m) suevites fall within the ranges for the upper impactite major element signatures.

Hydrothermal Alteration

In order to further constrain the extent of hydrothermal alteration, as indicated by the presence of secondary carbonate, a plot of LOI versus CaO contents was made (Fig. 2). In general, most of the samples have CaO contents in the range 0.5–3 wt% and LOI contents between 2 and 9 wt%. However, some outliers exist, and these high CaO contents correlate with high LOI contents. These high CaO contents together with high LOI values are evident in all lithologies throughout the core. If these signatures represent the effect of secondary carbonate precipitation from hydrothermal solutions, this indicates that hydrothermal alteration did take place throughout the whole LB-07A core (rather than in isolated lithologies). This is supported by petrographic characteristics (macroscopic and microscopic carbonate segregations, veins, and pods) (Coney et al. 2007). In this geochemical study, care was taken to separate any macroscopic carbonate pods from the samples crushed for geochemical analysis, and to ensure that the CaO results are representative of the bulk-rock composition rather than an artifact of random sampling of isolated carbonate-rich areas. However, it was impossible to separate thin (millimeter-wide) primary carbonate bands and small (<0.5 cm) carbonate pods that are present locally in the target rock, sometimes in significant amounts (up to 1.6 vol%) (Coney et al. 2007).

A small number of samples from all lithologies have high CaO and moderate LOI values and seemingly form a negative trend in Fig. 2. Whether or not this represents admixture of a further target rock component is not currently clear.

Table 2. Ranges for the major element contents the LB-07A lithologies, shale, graywacke-phyllite, Pepiakese granite, and Ivory Coast tektites of Koeberl et al. (1997, 1998); averages of the granite dikes and tektites are from Koeberl et al. (1997, 1998); and fallout suevites from Boamah and Koeberl (2003).

Overall range (wt%)	Polymict lithic breccia	Suevite	Monomict breccia	Basement metasediment (overall)	Granophyric lithology	Shale[a]	Graywacke-phyllite[a]	Granite dike (average)[a]	Pepiakese granite[a]	Tektites (average)[a]	Tektites[a]	Fallout suevite (average)[b]
SiO_2	46.4–66.2	53.8–70.0	56.0–77.0	49.7–78.3	51.2	53.56–57.21	63.30–69.12	68.74 ± 0.50	53.13–66.69	67.58 ± 0.59	66.2–68.5	63.58 ± 3.01
TiO_2	0.26–0.66	0.38–0.67	0.34–0.67	0.38–0.72	0.51	0.74–0.97	0.59–0.77	0.50 ± 0.00	0.06–0.88	0.56 ± 0.02	0.54–0.61	0.64 ± 0.07
Al_2O_3	6.0–17.7	5.0–17.0	10.9–19.0	10.4–18.6	12.1	17.68–22.62	12.70–17.02	15.91 ± 0.18	14.73–19.87	16.74 ± 0.37	16.3–17.7	15.58 ± 1.15
Fe_2O_3	3.3–7.5	4.7–7.5	3.0–7.4	3.4–7.1	7.2	7.99–9.14	5.64–7.57	3.97 ± 0.31	0.48–9.17	6.16 ± 0.15	5.8–6.5	6.58 ± 2.24
MnO	0.03–0.14	0.02–0.12	0.03–0.12	0.03–0.11	0.12	0.035–0.055	0.010–0.037	0.014 ± 0.013	0.001–0.106	0.06 ± 0.01	0.04–0.07	0.11 ± 0.05
MgO	1.5–15.0	1.6–12.7	1.3–4.4	1.2–9.3	6.8	2.40–3.31	1.79–2.50	1.44 ± 0.36	0.12–10.17	3.46 ± 0.35	3.0–4.4	1.43 ± 0.54
CaO	0.8–8.6	0.95–10.1	0.8–6.5	0.39–8.5	6.2	0.05–0.11	0.07–0.47	0.31 ± 0.01	0.23–6.76	1.38 ± 0.11	1.2–1.5	1.39 ± 0.61
Na_2O	0.9–3.8	0.11–5.4	1.3–4.5	0.36–3.6	1.5	0.36–2.13	0.31–3.07	4.14 ± 0.49	2.92–11.88	1.90 ± 0.16	1.5–2.1	1.73 ± 0.53
K_2O	d.l.–2.3	d.l.–2.5	0.57–2.9	0.83–5.2	1.2	2.64–3.07	0.85–2.72	1.92 ± 0.15	0.27–1.27	1.95 ± 0.11		1.27 ± 0.38
P_2O_5	0.05–0.14	0.04–0.37	0.06–0.14	0.03–0.22	0.15	0.04–0.13	0.02–0.10	0.06 ± 0.00	0.02–0.21			0.09 ± 0.03
LOI	3.6–17.2	2.7–15.1	2.1–4.9	2.7–13.9	12.3	6.86–8.99	3.49–5.32	2.98 ± 0.33	0.51–2.22			7.68 ± 2.22

[a]Data from Koeberl et al. (1997, 1998).
[b]Data from Boamah and Koeberl (2003).
d.l. = detection limit.

Fig. 2. CaO content versus LOI for the impactites and basement rocks of the LB-07A drill core.

There are two cases (polymict lithic breccia sample KR7-2 from a depth of 339.22 m and suevite sample KR7-6 from a depth of 360.65 m) where LOI contents are relatively high (>10 wt%) but CaO contents low (2 wt% or less). This implies that the total LOI values do not always relate only to CO_2, but other sources of secondary volatiles (e.g., SO_x from sulfide/sulfate, H_2O and hydroxide from primary target-rock minerals and secondary phyllosilicates) should be taken into consideration. Petrographic analysis (Coney et al. 2007) indicates that the LOI contents may be related to H_2O from alteration phases (e.g., chlorite, sericite) and other phyllosilicates, as these minerals are in evidence throughout the borehole. The two samples in which LOI contents are high but CaO contents are low contrast with the other samples with high LOI contents in that they have minor carbonate (<1 vol%) and abundant phyllite and mica-rich schist (>30 vol%) clasts.

Polymict Lithic Breccias versus Suevites

Similar ranges of abundances are seen for the lithic and suevitic breccias with respect to SiO_2, TiO_2, Al_2O_3, and CaO contents (higher maximum values for suevite samples). Both polymict breccia types have similar K_2O and Na_2O contents. More variation in Fe_2O_3 contents is observed in the lithic breccias as opposed to the suevites. Comparable variation is observed for the MgO contents in both polymict breccias, and this element shows the largest overall variation in the borehole. No correlation of the MgO content with the modal abundances of chlorite in metasediments can be made, and it is probable that a combination of minerals controls this geochemical signature.

Polymict Breccias (Upper Impactites) versus Monomict Breccias

The ranges in SiO_2 values of the monomict breccias are similar to those of the suevites, but are slightly higher on average. The TiO_2, CaO, and K_2O abundance ranges are the

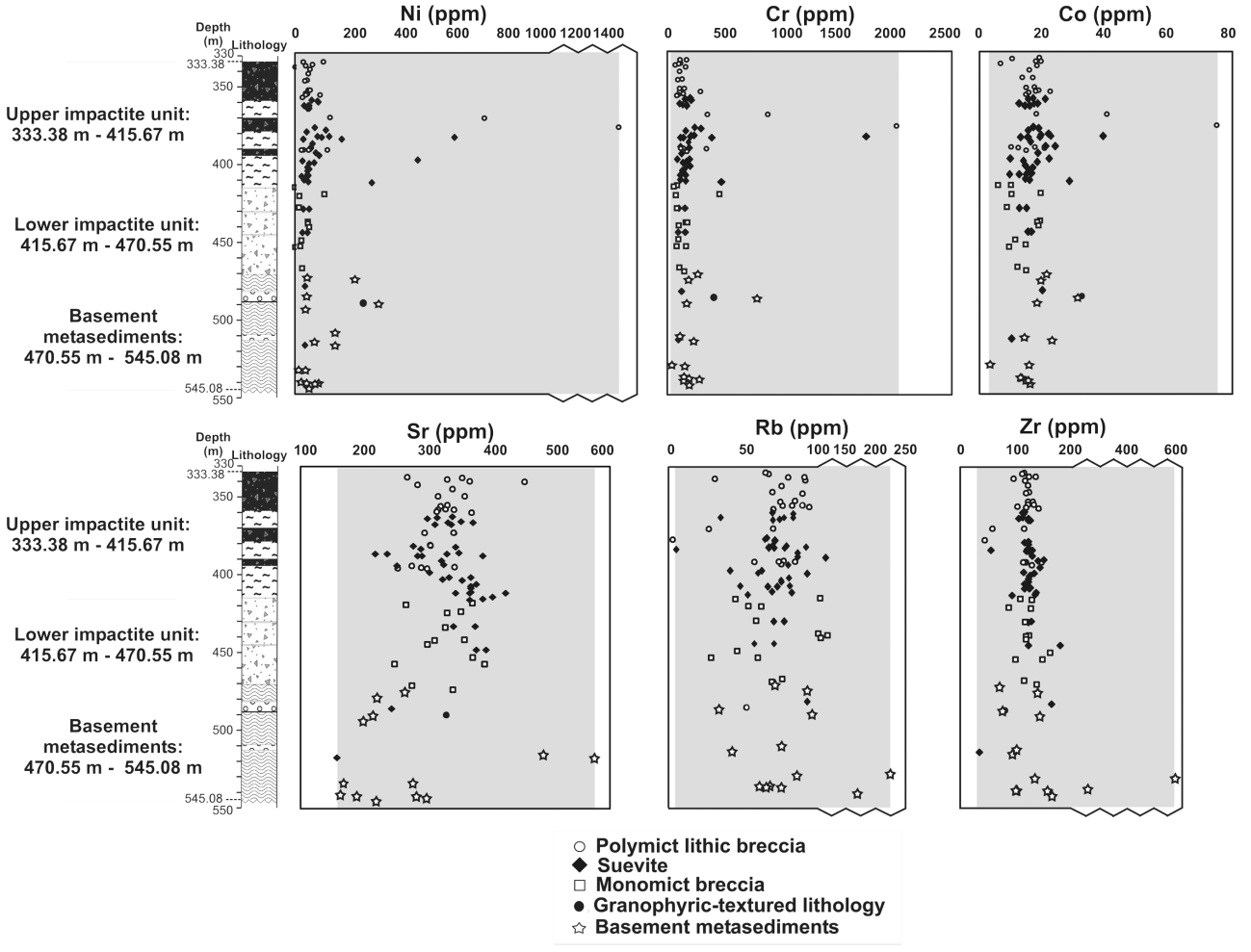

Fig. 3. Profiles of the abundances of Cr, Ni, Co, Rb, Sr, and Zr versus depth for the LB-07A drill core.

same for both the polymict and monomict breccias. The range in Al_2O_3 contents observed for the monomict breccias is similar to that of the upper impactites. The Na_2O contents vary within a smaller range for the monomict breccias than for the polymict breccias. Very little variation in the monomict breccias occurs in MgO contents compared to polymict breccias. Overall, there is more scatter in abundance values for the monomict breccias than for those of the polymict breccias.

Monomict Breccias versus Basement Lithologies

The SiO_2, Al_2O_3, CaO, and TiO_2 contents are similar for the monomict breccias and the basement lithologies. Abundances of Na_2O, K_2O, and MgO show comparatively wider scatter in the basement lithologies, whereas the Fe_2O_3 content has more scatter in the monomict breccias. Considering that both sequences are made up of the same lithologies, although locally at different proportions, this overall similarity is not surprising.

TRACE-ELEMENT CHARACTERISTICS

All eighty-six samples were analyzed by XRF and INAA for their trace-element content (Table 1). Selected trace-element values have been plotted against depth in Fig. 3. Niobium, Br, and Y values are generally either below the respective detection limits or are very low.

Polymict Lithic Breccias

The polymict lithic breccias show narrow ranges in concentration for Rb, Zr, Sr, and V. The range for V is larger than that observed for the suevites. Much scatter is seen for Ba. The chalcophile elements Zn and Cu show much scatter throughout the sequence. Nickel, Co, and Cr values vary within small intervals, and only two samples (at depths of 370.39 and 377.46 m) show high concentrations of up to 77 ppm Co, 1418 ppm Ni, and 2023 ppm Cr. These samples also show substantial enrichments in As (401 ppm and 728 ppm, respectively). There is no corresponding

enrichment in the Zn concentrations; however, Sb values for both samples are higher than the typical range observed for the lithic breccias (Table 1). These enrichments might be caused by the presence of accessory arsenopyrite or other sulfide minerals. As this section of core is essentially powderized, no representative thin sections could be evaluated. However fine-grained opaque minerals (less than 50 μm in size) have been noted in thin section, the identity of which has not been resolved yet due to small size. The siderophile element variation patterns of Ni, Cr, and Co are similar to each other (Fig. 3).

Suevites

The suevites have geochemical signatures that are similar to those of the lithic breccias. Little variation is seen for Rb, Zr, and V values, with much scatter observed in Sr, Ba, Zn, and Cu values (Table 1). As with the lithic breccias, the Ni, Co, and Cr contents are positively correlated, and only a few outliers with very high Ni and Co abundances (up to 605 ppm Ni and 31 ppm Co) are observed (at depths of 383.74 m, 398.44 m, and 413.13 m). The suevite at a depth of 383.74 m also has high As values (of 159 ppm) and somewhat enriched Sb values (0.74 ppm). This sample contains a number of highly oxidized shale clasts, which contain microscopic sulfides (most likely pyrite and chalcopyrite, though due to their small size this has not yet been fully evaluated).

Monomict Breccias

The monomict breccias show less variation in Rb, Sr, and Zr concentrations (Rb: 29–107 ppm; Sr: 259–394 ppm; Zr: 89–162 ppm) than the upper impactite polymict breccias (Rb: 33–92 ppm; Sr: 191–413 ppm; Zr: 45–150 ppm). The monomict breccias have no substantially elevated concentrations in the siderophile elements, and very little variation is observed throughout this part of the sequence (see Fig. 3). The range for V is the largest seen throughout the core. No enrichment in the As, Sb, or Zn concentrations is observed for any of the monomict breccia samples, in comparison to the polymict lithic breccias and suevites (Table 1).

Basement Lithologies

The basement lithologies show the most scatter for Rb, Sr, Zr, Ba, and Y out of all the lithologies analyzed. Rubidium, Ba, and Cs show the highest concentrations in the borehole in the basement lithologies, which potentially correspond to a local enrichment in feldspar (e.g., Rollinson 1993), although owing to the disaggregated state of the core this cannot be conclusively confirmed. One sample contains a substantial relative enrichment in Zr (580 ppm, from an average range of ~90–150 ppm), coincident with elevated Ba, Y, and Hf concentrations, and this most likely represents random sampling of zircon or other accessory minerals, although again this cannot be conclusively confirmed; zircon has been noted throughout this study only rarely. Vanadium concentrations are variable, similarly to the polymict breccias. Arsenic concentrations are rarely above 25 ppm, and Sb contents are generally low (<0.3 ppm).

Granophyric-Textured Lithology

The granophyric-textured lithology is characterized by higher Ni, Cr, Co, and As than the majority of the LB-07A samples. The lithophile element abundances of Rb, Sr, Zr, and V are all within the range of the impactites.

Siderophile Elements and Possible Meteoritic Component

Chromium, Co, and Ni abundances generally have narrow ranges, with just a few samples showing relative enrichments. For Ni, the range typically lies between 6 and 200 ppm, with a maximum concentration of 1122 ppm. The highest concentrations of Ni (200–1122 ppm) occur within the polymict breccias of the upper impactite (Fig. 3), and the maximum concentration corresponds to a sample that has a higher concentration of Fe_2O_3 than most other samples, and is intensely iron-stained. A number of samples within the range of 200–1122 ppm concentration of Ni contain a substantial proportion of melt particles. However, for other melt-rich units, such as the suevite intercalation at a depth of 430.13 m (up to 18 vol% melt locally) (Coney et al. 2007), very little enrichment in Ni is observed. No substantial and consistent differences in Ni concentration between the lithic breccias and the suevites have been noted, as similar numbers of lithic and suevitic breccias have high Ni concentrations. Great variation in Ni concentrations is also observed in the basement rocks, predominantly in the meta-graywacke samples and the granophyric-textured rock from a depth of 487.12 m. The Co and Cr patterns are similar to the Ni pattern. Maximum enrichment in both Co and Cr concentrations (up to 2023 ppm and 77 ppm, respectively) coincides with maximum Ni enrichment. The average Co concentrations are between 3 and 20 ppm. The Cr values lie in the range of 50–200 ppm. Copper concentrations correlate positively with the Cr, Co, and Ni concentrations (and a number of these samples also have high As contents up to 728 ppm), which is a strong indication that sulfide, especially the secondary sulfides such as pyrite, arsenopyrite, and chalcopyrite, whose presence is indicated from the petrographic studies (see Coney et al. 2007), is responsible for the local enrichment of these elements. All iridium results by INAA are below the detection limit of ~2 ppb for carbonate-poor samples and ~0.5 ppb for carbonate-rich samples.

A number of samples, especially those enriched in Ni, Cr, and Co, were analyzed for their platinum group element contents in order to ascertain whether a meteoritic component could be detected. The results are discussed by McDonald et al. (2007). In essence, no definitive evidence for the presence of a meteoritic component was obtained in any of these samples.

Rare Earth Element Data

Rare earth element (REE) data were obtained for 60 samples using INAA (Fig. 4). The REE concentrations were normalized to the composition of C1 chondrites after Taylor and McLennan (1985) and selected patterns are shown in Figs. 4a–d. The impactites have very similar normalized REE abundances to each other (Figs. 4a–d). The normalized data range for most of the samples is similar to values given by Koeberl et al. (1998).

The light REE are consistently significantly enriched (Figs. 4a–d), and weak negative Eu anomalies are present. Most calculated Eu anomaly values (Eu/Eu*) are less than 1. Selected samples show very weak negative Ce anomalies. Koeberl et al. (1998) found that their shale, graywacke, and phyllite samples displayed slight negative Eu and Ce anomalies, and this agrees with the observations made in the present study. One basement rock sample of our suite (from a depth of 530.63 m) showed significantly higher REE abundances (Fig. 4d), and this sample also showed enrichment in K_2O, as well as Zr, Hf, and U, which could mean that the sample is enriched in zircon, as hypothesized in the Basement Lithologies section. Unfortunately, only a powder mount of this sample could be examined, and the only rock fragments in evidence are altered shale, meta-graywacke, and a little carbonate. No distinct differences were noted with increasing depth, or between the three sequences. When the ratios of La/Th (Fig. 4e) and La/Lu (Fig. 4f) are plotted with depth, for both ratios some scatter is observed; average values are La/Lu ~6 and La/Th ~70. The suevites of the upper impactite and the lower impactite sequences are not different with respect to their REE signatures; the suevites from the basement rock sequence have yet to be fully analyzed for their REE component.

DISCUSSION

Geochemical Characteristics of the LB-07A Borehole

The major- and trace-element patterns throughout the LB-07A borehole are, overall, fairly constant with depth. The following trends can be noted:

- CaO values vary throughout the borehole, and this is thought to reflect hydrothermal alteration in addition to the presence of carbonate target rock, as discussed by Coney et al. (2007).
- The basement lithologies show the most variation in range of many of the major elements as well as in the trace-element concentrations.
- Although a number of samples are enriched in siderophile elements, further analysis has not revealed the presence of a meteoritic component (McDonald et al. 2007).

The suevites and the lithic breccias of the LB-07A borehole do not seem to be chemically distinct from each other, and are not substantially different from the average compositions of the monomict breccias and basement rock lithologies (Table 2), indicating that extensive homogenization has taken place (Fig. 1; Table 1). Dressler and Reimold (2001) discussed how homogenization of the target rock material in impactites is a common observation. This has also been observed for corrected geochemical trends in the Yax-1 drill core of the Chicxulub structure (e.g., Tuchscherer et al. 2004). However, unlike in the Bosumtwi core, slightly differing chemical characteristics could be detected for the different lithostratigraphic units (e.g., Schmitt et al. 2004) of that drill core.

For a number of the major and trace elements, the scatter in the range of composition increases with depth within the basement lithologies (no obvious difference can be ascertained between the upper and lower impactites). This provides further evidence for extensive mixing of the target lithologies for the polymict and monomict breccias.

In terms of the petrographic signature of the LB-07A borehole, our results (Coney et al. 2007) show that the overall composition of the LB-07A borehole is 43.6% meta-graywacke, 40.9% shale, 5.9% phyllite, 4.8% quartz, and 1.6% carbonate. In terms of relative proportions, meta-graywacke and shale are similar and dominate the petrographic signature. Thus, it can be concluded that much of the geochemical signature will reflect these lithologies. The petrographic study (Coney et al. 2007) also showed that there is much fluctuation in clast composition and, locally, in relative clast proportion, which influences the geochemical signature of the polymict breccia samples.

In order to examine a possible clast control on major element content, the volume percentage of shale was compared to the Fe_2O_3 and MgO contents. It was noted that in only a few samples with high volume percentages of shale (in comparison to meta-graywacke and other lithic components), there was a weak correlation with high concentrations of Fe_2O_3 and MgO. The majority of shale-rich samples lie in small ranges for both Fe_2O_3 and MgO contents, and no defining correlation can be made. Thus, shale contents are not the sole control of Fe_2O_3 and MgO contents and other minerals must influence the geochemical signature. It is possible that, in addition to minerals such as the phyllosilicates, another factor may be involved, such as the matrix composition. Further work is currently in progress to examine this possibility.

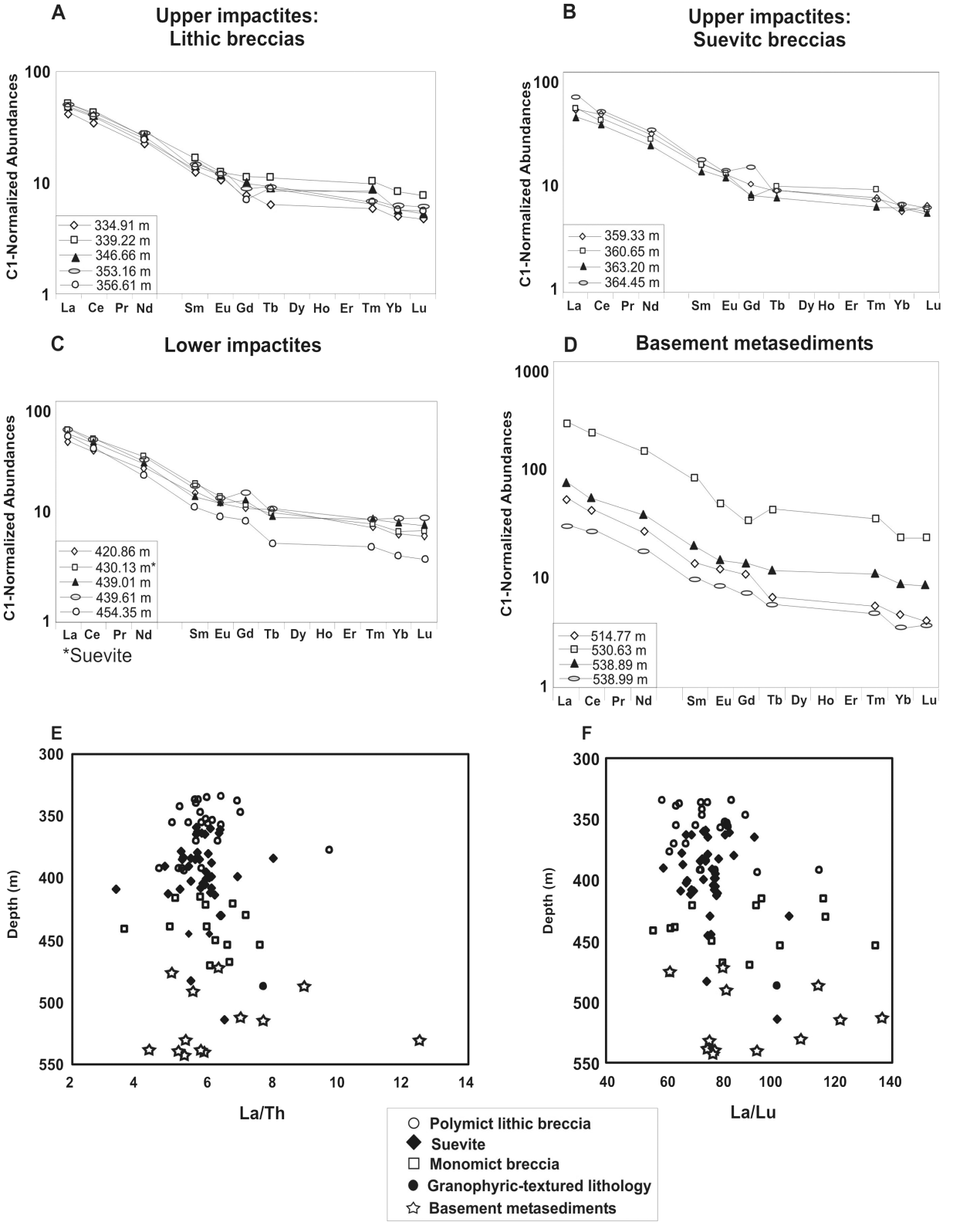

Fig. 4. Selected C1 chondrite-normalized rare earth element patterns (normalization factors after Taylor and McLennan 1985). a) Upper impactite lithic breccias. b) Upper impactite suevitic breccias. c) Lower impactite. d) Basement lithologies. e) La/Th ratios for all samples. f) La/Lu ratios for all samples.

Vanadium concentrations vary widely throughout the borehole, and this is most likely due to the variation in biotite as well as rutile. In order to test for substitution of V in rutile, a plot of Ta versus V was made (as V substitution in Ta-rich varieties of rutile is common), and correlation is apparent.

No distinct changes potentially related to alteration are evident for the monomict breccias of the lower impactites. This is consistent with the local origin of the breccias and that their compositions reflect original lithologies that would have been as diverse as the basement rock below. It is apparent that little hydrothermal alteration has taken place in the monomict breccias, and that these brecciated rocks were not necessarily a channel for carbonate-rich fluids, indicating that the origin of the fluids was potentially from above, rather than from below the polymict breccias.

Unlike the impactites of the Yax-1 drill core from the Chicxulub structure (e.g., Schmitt et al. 2004), the K_2O content in this Bosumtwi sequence is nearly always less than, or the same as, the average continental crust value of 2.6 wt% (Wedepohl 1995). Schmitt et al. (2004) used the observation of high K_2O contents to suggest that potassium metasomatism, caused by postimpact hydrothermal alteration, had taken place in the Yax-1 impactites. Only one sample in the Bosumtwi rocks shows an elevated concentration of K_2O (which may indicate the presence of K-feldspar); thus, conclusive evidence for potassium metasomatism has not been found. The majority of feldspar observed in the LB-07A borehole is plagioclase, rather than K-feldspar (Coney et al. 2007).

Coney et al. (2007) suggest that the granophyric lithology may be a hydrothermally altered vein of the regionally occurring granophyric granitoid lithology that was first described by Reimold et al. (1998). The LOI of this sample is particularly high, with a value of 12.30 wt%, and is correlated with a high content of CaO (6.82 wt%). In petrographic examination, it was found that this sample contained extensive carbonate, quartz-feldspar intergrowth, and muscovite (see Coney et al. 2007). Also noted was sericitized plagioclase, which would have been produced by hydrothermal alteration. The granophyric-textured lithology also contains significant abundances of Fe_2O_3 and MgO, and these can be accounted for by the abundant mica minerals.

In terms of comparing the degree of alteration of the different suevites throughout the borehole, it has been observed that the lowermost basement suevite has a substantially different major- and trace-element signature compared to the other suevites in the core, including the other suevite injection in the basement. For example, the trace-element geochemical signature of the lowermost basement suevite shows substantially lower Ba, Sr, and V concentrations in comparison to the uppermost basement suevite as well as the lower impactite suevites. The uppermost suevite has higher Rb and Zn and lower Sr concentrations than the lower impactite suevites. The suevites in the lower impactites have very similar major- and trace-element signatures to each other, and have major- and trace-element compositions intermediate to the range seen in the upper impactites. The most notable difference between the upper and lower impactite suevites is that the upper impactites show higher average Co values, and contain the highest Ni and Cr concentrations of all suevites. It was noted in the petrographic study (Coney et al. 2007) that the color of the melt particles and the matrices of the suevites varied throughout the core, changing from gray-brown in the upper impactites to greenish yellow in the lower impactites and either lighter or darker gray in the basements intercalations. Changes in the mineralogy of the suevites were found (Coney et al. 2007), but it is most likely that the matrices of the suevites may provide more evidence of alteration. This work is in progress.

Major-Element and Trace-Element Signatures of the LB-07A Impactites versus those of Target Rocks

Koeberl et al. (1998) calculated average compositions of their identified target rocks for the Bosumtwi structure (shale, phyllite-graywacke, granite dikes, and the Pepiakese granite) (Table 2). In comparing the ranges of these rocks, a number of differences are apparent.

Basement Metasediments versus Target Rock Types

A total of 14 LB-07A basement samples were analyzed, and these are compared to the ranges (Table 2) quoted for the shales and graywacke-phyllites identified by Koeberl et al. (1998). The LB-07A meta-graywacke was found to have an overall similar signature to the graywacke-phyllite of Koeberl et al. (1998), with the following exceptions: the meta-graywacke shows slightly higher concentrations of MnO, MgO, P_2O_5, and LOI, and a significantly higher content of CaO. The LB-07A meta-graywacke also has slightly lower concentrations of SiO_2, TiO_2, and Fe_2O_3, and similar concentrations of Al_2O_3, Na_2O, and K_2O in comparison with the graywacke-phyllites. Thus, the only significant difference between the LB-07A meta-graywacke and those of Koeberl et al. (1998) is the CaO content. The LB-07A altered shales are more similar in composition to the shale compositions of Koeberl et al. (1998) than the meta-graywackes are to the graywacke-phyllites, but the shales generally have larger ranges than those quoted by Koeberl et al. (1998), namely for SiO_2, MnO, MgO, P_2O_5, K_2O, and Na_2O. Lower concentrations were observed for TiO_2 and Fe_2O_3 and enrichments in CaO and LOI exist. Both the meta-graywackes and altered shales of LB-07A have substantially higher CaO (together with high LOI) contents than the shales and graywacke-phyllites, providing evidence for a substantial carbonate component, which is both of primary and secondary origin (see Coney et al. 2007).

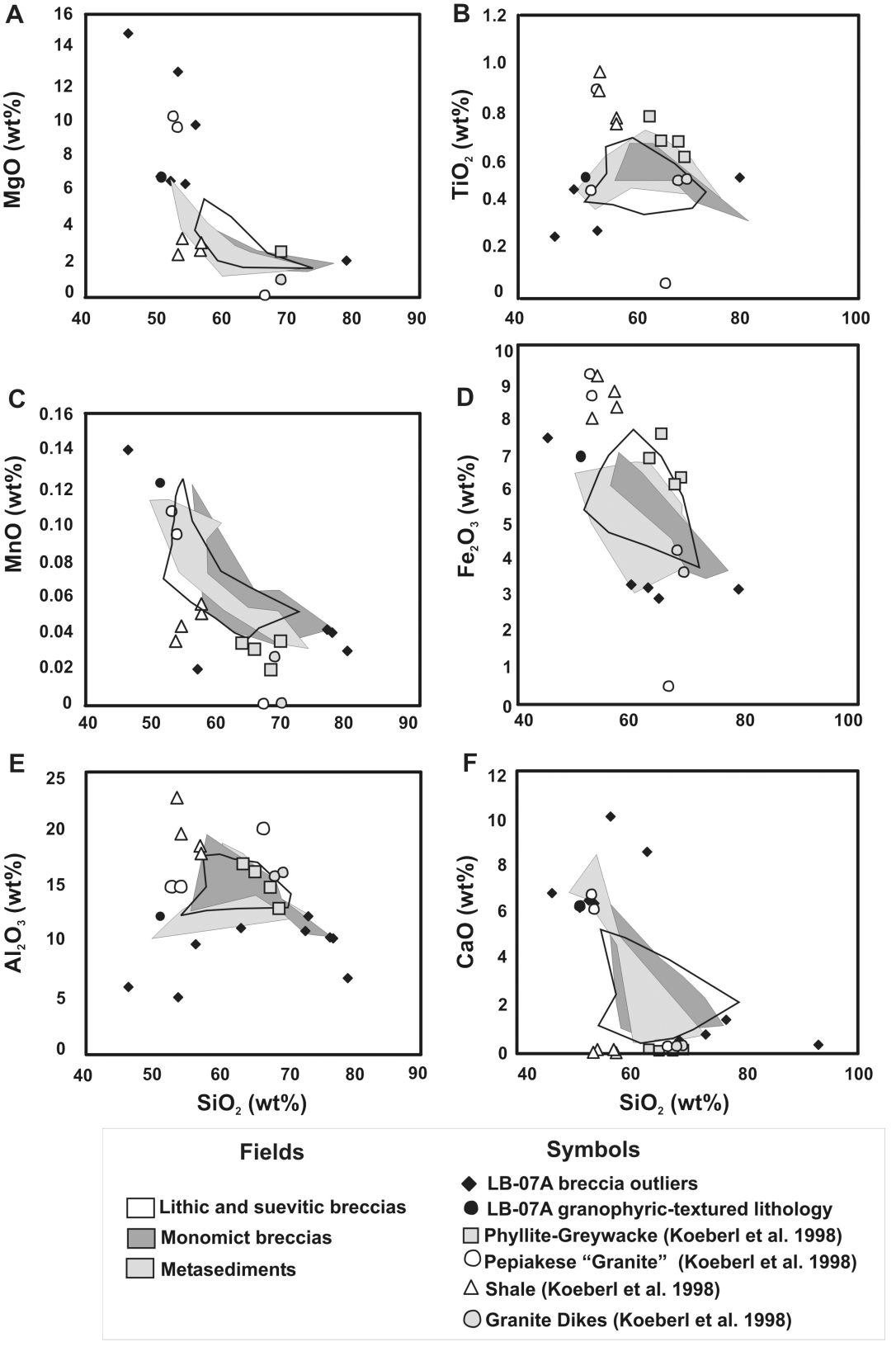

Fig. 5. Harker diagrams showing the major-element fields for the polymict breccias, monomict breccias, and basement metasediments of the LB-07A borehole, compared with target rock values from Koeberl et al. (1998).

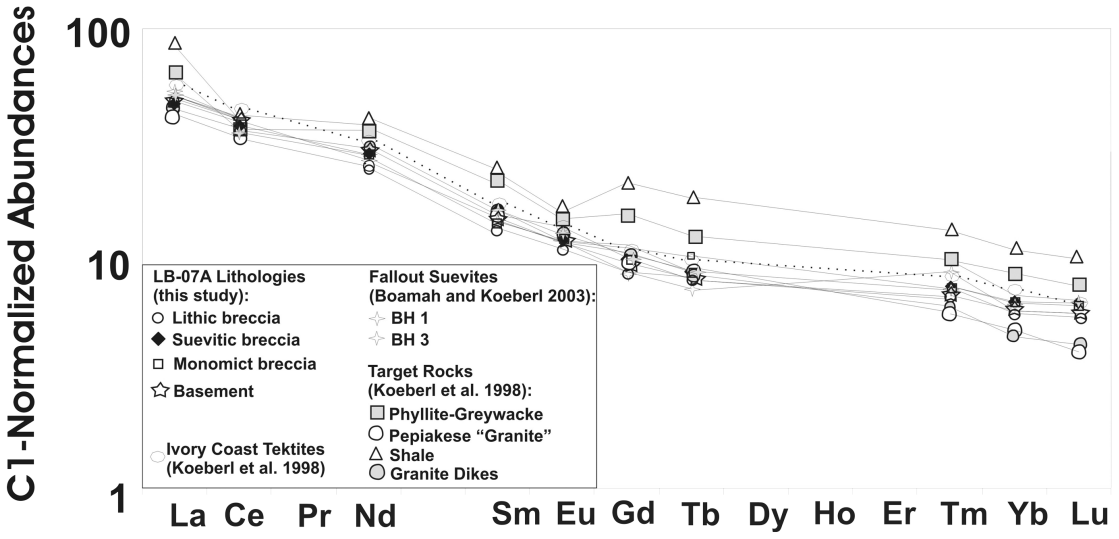

Fig. 6. C1 chondrite-normalized rare earth element patterns (normalization factors after Taylor and McLennan 1985) comparing average rare earth element patterns of the upper impactite lithic breccias, upper impactite suevitic breccias, lower impactites, and basement lithologies with the average fallout suevites (Boamah and Koeberl 2003), as well as the average target rocks and Ivory Coast tektites (data from Koeberl et al. 1998).

Polymict/Monomict Breccias versus Target Rocks

Harker plots of the impactite compositions (Fig. 5) show that the impactites and basement rocks of the LB-07A borehole consist of a thoroughly homogenized mixture of target rocks similar to those analyzed by Koeberl et al. (1998). However, an additional lithology must be involved (particularly noticeable for Fe_2O_3, CaO, and MnO contents), as a number of samples have outliers that are more enriched in those elements than the general field defined by the majority of samples. The fields that delineate the monomict breccias, the basement metasediments, and the majority of the polymict breccias mirror each other in shape and extent, showing that the LB-07A column is reasonably well homogenized in terms of the geochemical signature. The most notable difference between the LB-07A impactite concentrations and the target rocks is that they are generally more enriched in CaO than the target samples, except for the Pepiakese granite. Of course, this discrepancy could also be due to the small number of target rock samples analyzed so far from the Bosumtwi region (see also Karikari et al. 2007).

Major Element Signatures for LB-07A Suevites versus the Ivory Coast Tektites

The major element compositions of Ivory Coast tektites (Table 2; see also Koeberl et al. 1997, 1998) are compared here to the suevites of the LB-07A core, as these two rock types should represent mixed compositions of the target rocks. The tektites always have narrower compositional ranges than the LB-07A suevites. In general, the tektite major-element range is within the range for the suevites, indicating that they were derived from the same target rocks, but that comparably less homogenization has taken place in the suevites. There are two main differences between the suevites and the tektites: the MgO and CaO contents of the suevites are much higher than those for the tektites. The larger range may well reflect that the suevites show evidence for postimpact alteration.

Major-Element Signatures for the LB-07A Suevites versus the Fallout Suevites

The major-element signatures for the LB-07A suevites are very similar to the averages measured by Boamah and Koeberl (2003) (Table 2). The average abundances in fallout suevites for SiO_2, TiO_2, Al_2O_3, Fe_2O_3, MnO, Na_2O, K_2O, CaO, P_2O_5, and the LOI all are within the range of the LB-07A suevites. The CaO value for the fallout suevites lies toward the minimum values for the LB-07A suevites (1.38 wt% versus a maximum of 10.1 wt%). The only exception is the MgO content, which is lower in the fallout suevites (1.43 wt%) in comparison to the LB-07A suevite range of 1.6–12.7 wt%, and this may well reflect postimpact alteration as seen in the comparison with the tektites.

Average Trace-Element Signatures of the LB-07A Rocks versus Target Rocks, Fallout Suevites, and the Ivory Coast Tektites

In order to further compare the geochemical signatures of the impactites and basement rocks of LB-07A, a plot of the C1-normalized REE signatures for the averages of the different lithologies in LB-07A is compared to the averages for the four target lithologies (phyllite-graywacke, granite dikes, shale, and Pepiakese granite), fallout suevites, and Ivory Coast tektites of Koeberl et al. (1998) and presented in Fig. 6. Additionally, two ternary plots of Th-Hf-Co and La-Cr-Sc for the averages of these lithological types are

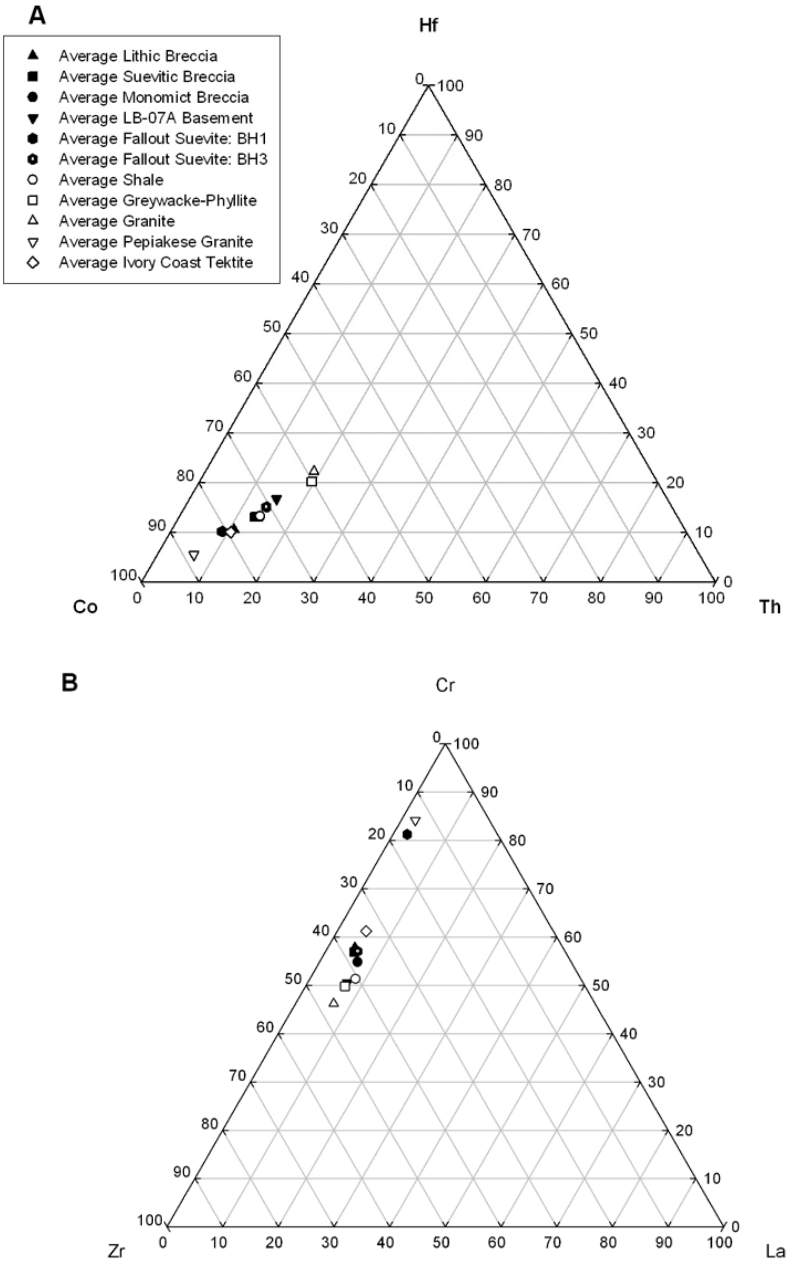

Fig. 7. Ternary plots of (a) Th-Hf-Co and (b) La-Cr-Zr for averages for the LB-07A lithic, suevitic, and monomict breccias, and basement rocks, together with the average fallout suevites from boreholes BH1 and BH3 (Boamah and Koeberl 2003), and averages for the target rocks and Ivory Coast tektites (Koeberl et al. 1998).

shown in Fig. 7. As noted in the Rare Earth Element Data section, the impactites have very similar normalized REE abundances to each other (Figs. 4a–d and 6). These normalized abundances, however, are slightly lower than those for the average shale and graywacke-phyllites. Furthermore, the Pepiakese granite has lower abundances than the LB-07A rocks; the fallout suevites are close in value to the LB-07A rocks although the values from borehole 1 (BH1) (Boamah and Koeberl 2003) are closer to the graywacke-phyllites. The average granite, however, has intermediate composition, which is comparable to the LB-07A lithologies. Thus, the REE normalized abundances are intermediate to those of the target rocks, as expected from previous results.

The ternary plots (Fig. 7a) show similar features: the LB-07A lithologies lie on apparent “tie-lines” between the different target rocks. For the first plot, Th-Hf-Co, the end-points of the tie-line are an average granite together with graywacke-phyllite and the average Pepiakese granite. In this case, shale is in the middle of the tie-line defining the field,

and the Ivory Coast tektites show similar compositions to fallout suevites from BH1. A similar relationship is also indicated by the La-Cr-Zr ternary plot (Fig. 7b) and the end-points are the same as in the other ternary plot. Thus, it is apparent that the LB-07A rocks are most similar in composition to the graywacke-phyllite and shale components, but are intermediate to the granite dikes and the Pepiakese granite. This is in agreement with the petrographic data (Coney et al. 2007), which indicates that most of the samples are composed chiefly of meta-graywacke and altered shale.

CONCLUSIONS

Thirty-six samples of suevite, 36 samples of lithic and monomict breccia, and 14 samples of meta-graywacke and shale (target rocks) from drill core LB-07A in the crater moat around the central uplift of the Bosumtwi impact structure were analyzed for their major- and trace-element compositions. From comparison of the geochemical signatures of impactites and basement rocks from the LB-07A drill core, we draw the following conclusions:

- The major-element compositions of the LB-07A core are fairly uniform in range with respect to depth, irrespective of rock type, with the exception of CaO, MgO, and Fe_2O_3. This suggests that the silicate component of the impactites has been relatively well homogenized. However, there is much variation in the amount of scatter with depth, and in general scatter increases with depth (except notably for TiO_2). Any variability is likely a function of differences in the population of small clasts (<1 cm). This aspect needs to be studied further.
- The LB-07A polymict and monomict breccias generally have compositions intermediate to those target rock components analyzed by Koeberl et al. (1998), but an additional source of Fe_2O_3, CaO, and MnO is apparent. For the CaO, it is likely that this corresponds to a separate carbonate component, as noted by Coney et al. (2007).
- The LB-07A basement metasediments are very similar in composition to the target rocks of Koeberl et al. (1998), with larger ranges observed for the altered shales of the LB-07A core. Higher CaO and LOI values are noted for both LB-07A metasediments in comparison to the target rocks.
- Trace-element abundances are strongly controlled by the compositions of the graywacke-phyllites and shales.
- The Ivory Coast tektites have narrower major-element ranges than those for the suevites, but overlap in the compositional ranges is apparent. The suevites have far larger ranges for MgO and CaO than the tektites, and this may have been caused by post-impact alteration.
- The major-element composition for the fallout suevites is very similar to the LB-07A suevites, except for MgO values.
- Overall limited hydrothermal alteration is clearly indicated by locally elevated CaO and LOI values. This is also indicated by the petrographic study, where both primary as well as secondary carbonate was in evidence. The hydrothermal alteration is not restricted to a particular depth or lithology, and is apparent throughout the core.
- LOI values are not solely controlled by CaO contents, and most likely also involve H_2O from primary and secondary phyllosilicates.
- The contents of the siderophile elements do not indicate the presence of a significant meteoritic component in the impactites.

Acknowledgments–Drilling at Bosumtwi was supported by the International Continental Drilling Program (ICDP), the U.S. NSF-Earth System History Program under grant #ATM-0402010, Austrian FWF (project #P17194-N10), the Austrian Academy of Sciences, and the Canadian NSERC. Drilling operations were performed by DOSECC. The present work is funded through a grant from the National Research Foundation (NRF) of South Africa (to W. U. R. and R. L. G.), a Scarce-Skills Bursary from the NRF (to L. C.), a Jim and Gladys Taylor Trust award (to L. C.), and an Austrian Science Foundation (FWF) grant (project #P17194-N10 to C. K.). Sharon Turner, University of the Witwatersrand, and Ralf Schmitt, Humboldt University, are thanked for XRF analyses, and Dieter Mader, University of Vienna, is thanked for assistance with the INAA analyses. J. Morrow and D. King are thanked for constructive reviews. This work forms part of L. Coney's Ph.D. thesis. This is University of the Witwatersrand Impact Cratering Research Group Contribution No. 102.

Editorial Handling—Dr. Bernd Milkereit

REFERENCES

Boamah D. and Koeberl C. 2002. Geochemistry of solids from the Bosumtwi impact structure, Ghana. In *Meteorite impacts in Precambrian shields,* edited by Plado J. and Pesonen L. J. Impact Studies, vol. 2. Heidelberg: Springer-Verlag. pp. 211–255.

Boamah D. and Koeberl C. 2003. Geology and geochemistry of shallow drill cores from the Bosumtwi impact structure, Ghana. *Meteoritics & Planetary Science* 38:1137–1159.

Boamah D. and Koeberl C. 2006. Petrographic studies of "fallout" suevite from outside the Bosumtwi impact crater, Ghana. *Meteoritics & Planetary Science* 41:1761–1774.

Coney L., Gibson R. L., Reimold W. U., and Koeberl C. 2007. Lithostratigraphic and petrographic analysis of ICDP drill core LB-07A, Bosumtwi impact structure, Ghana. *Meteoritics & Planetary Science* 42. This issue.

Dai X., Boamah D., Koeberl C., Reimold W. U., Irvine G., and McDonald I. 2005. Bosumtwi impact structure, Ghana: Geochemistry of impactites and target rocks, and search for a meteoritic component. *Meteoritics & Planetary Science* 40: 1493–1511.

Davis D. W., Hirdes W., Schaltegger U., and Nunoo E. A. 1994. U-Pb age constraints on deposition and provenance of Birimian and gold-bearing Tarkwaian sediments in Ghana, West Africa. *Precambrian Research* 67:89–107.

Dressler B. O. and Reimold W. U. 2001. Terrestrial impact melt rocks and glasses. *Earth Science Reviews* 56:205–284.

Jones W. B. 1985. Chemical analyses of Bosumtwi crater target rocks compared with Ivory Coast tektites. *Geochimica et Cosmochimica Acta* 49:2569–2576.

Ferrière L., Koeberl C., and Reimold W. U. 2007a. Drill core LB-08A, Bosumtwi impact structure, Ghana: Petrographic and shock metamorphic studies of material from the central uplift. *Meteoritics & Planetary Science* 42. This issue.

Ferrière L., Koeberl C., Reimold W. U., and Mader D. 2007b. Drill core LB-08A, Bosumtwi impact structure, Ghana: Geochemistry of fallback breccia and basement samples from the central uplift. *Meteoritics & Planetary Science* 42. This issue.

Gentner W., Kleinmann B., and Wagner G. A. 1967. New K-Ar and fission track ages of impact glasses and tektites. *Earth and Planetary Science Letters* 2:83–86.

Glass B. P., Kent D. V., Schneider D. A., and Tauxe L. 1991. Ivory Coast microtektite strewn field: Description and relation to the Jaramillo geomagnetic event. *Earth and Planetary Science Letters* 107:182–196.

Hirdes W., Davis D. W., Lüdtke G., and Konan G. 1996. Two generations of Birimian (Paleoproterozoic) volcanic belts in northeastern Côte d'Ivoire (West Africa): Consequences for the "Birimian Controversy." *Precambrian Research* 80:173–191.

Junner N. R. 1937. The geology of the Bosumtwi caldera and surrounding country. *Gold Coast Geological Survey Bulletin* 8: 1–38.

Karikari F., Ferrière L., Koeberl C., Reimold W. U., and Mader D. 2007. Petrography, geochemistry, and alteration of country rocks from the Bosumtwi impact structure, Ghana. *Meteoritics & Planetary Science* 42. This issue.

Koeberl C. 1993. Instrumental neutron activation analysis of geochemical and cosmochemical samples: A fast and proven method for small sample analysis. *Journal of Radioanalytical and Nuclear Chemistry* 168:47–60.

Koeberl C. 1994. Neutron activation analysis. In *Methods and instrumentations: Results and recent developments,* edited by Marfunin A. S. Advanced Mineralogy, vol. 2. Berlin: Springer Verlag. pp. 322–329.

Koeberl C. and Shirey S. B. 1993. Detection of a meteoritic component in Ivory Coast tektites with rhenium-osmium isotopes. *Science* 261:595–598.

Koeberl C. and Reimold W. U. 2005. Bosumtwi impact crater, Ghana (West Africa): An updated and revised geological map, with explanations. *Jahrbuch der Geologischen Bundesanstalt, Wien (Yearbook of the Austrian Geological Survey)* 145:31–70 (+1 map, 1:50,000).

Koeberl C., Bottomley R. J., Glass B. P., and Storzer D. 1997. Geochemistry and age of Ivory Coast tektites and microtektites. *Geochimica et Cosmochimica Acta* 61:1745–1772.

Koeberl C., Reimold W. U., Blum J. D., and Chamberlain C. P. 1998. Petrology and geochemistry of target rocks from the Bosumtwi impact structure, Ghana, and comparison with Ivory Coast tektites. *Geochimica et Cosmochimica Acta* 62:2179–2196.

Koeberl C., Milkereit B., Overpeck J. T., Scholz C. A., Peck J., and King J. 2005. The 2004 ICDP Bosumtwi impact crater, Ghana, West Africa, drilling project: A first report (abstract #1830). 36th Lunar and Planetary Science Conference. CD-ROM.

Koeberl C., Milkereit B., Overpeck J. T., Scholz C. A., Reimold W. U., Amoako P. Y. O., Boamah D., Claeys P., Danuor S., Deutsch A., Hecky R. E., King J., Newsom H., Peck J., and Schmitt D. R. 2006. An international and multidisciplinary drilling project into a young complex impact structure: The 2004 ICDP Bosumtwi impact crater, Ghana, drilling project—An overview (abstract #1859). 37th Lunar and Planetary Science Conference. CD-ROM.

Kolbe P., Pinson W. H., Saul J. M., and Miller E. W. 1967. Rb-Sr study on country rocks of the Bosumtwi crater, Ghana. *Geochimica et Cosmochimica Acta* 31:869–875.

Lacroix A. 1934. Sur la découverte de tektites à la Côte d'Ivoire. *Comptes Rendus de l'Academie des Sciences Paris* 199:1539–1542.

Leube A., Hirdes W., Mauer R., and Kesse G. O. 1990. The Early Proterozoic Birimian Supergroup of Ghana and some aspects of its associated gold mineralization. *Precambrian Research* 46: 136–165.

McDonald I., Peucker-Ehrenbrink B., Coney L., Ferrière L., Reimold W. U., and Koeberl C. 2007. Search for a meteoritic component in drill cores from the Bosumtwi impact structure, Ghana: Platinum-group element contents and osmium isotopic characteristics. *Meteoritics & Planetary Science* 42. This issue.

Oberthür T., Vetter U., Davis D. W., and Amanor J. A. 1998. Age constraints on gold mineralization and Palaeoproterozoic crustal evolution in the Ashanti belt of southern Ghana. *Precambrian Research* 89:129–143.

Palme H., Janssens M.-J., Takahashi H., Anders E., and Hertogen J. 1978. Meteorite material at five large impact craters. *Geochimica et Cosmochimica Acta* 42:313–323.

Plado J., Pesonen L. J., Koeberl C., and Elo S. 2000. The Bosumtwi meteorite impact structure, Ghana: A magnetic model. *Meteoritics & Planetary Science* 35:723–732.

Reimold W. U., Koeberl C., and Bishop J. 1994. Roter Kamm impact crater, Namibia: Geochemistry of basement rocks and breccias. *Geochimica et Cosmochimica Acta* 58:2689–2710.

Reimold W. U., Brandt D., and Koeberl C. 1998. Detailed structural analysis of the rim of a large, complex impact crater: Bosumtwi crater, Ghana. *Geology* 26:543–546.

Rollinson H. 1993. *Using geochemical data: Evaluation, presentation, interpretation.* London: Longman Group UK Limited. 352 p.

Schmitt R. T., Wittmann A., and Stöffler D. 2004. Geochemistry of drill core samples from Yaxcopoil-1, Chicxulub impact crater, Mexico. *Meteoritics & Planetary Science* 39:979–1001.

Schnetzler C. C., Pinson W. H., and Hurley P. M. 1966. Rubidium-strontium age of the Bosumtwi crater area, Ghana, compared with the age of the Ivory Coast tektites. *Science* 151:817–819.

Schnetzler C. C., Philpotts J. A., and Thomas H. H. 1967. Rare earth and barium abundances in Ivory Coast tektites and rocks from the Bosumtwi crater area, Ghana. *Geochimica et Cosmochimica Acta* 31:1987–1993.

Shaw H. F. and Wasserburg G. J. 1982. Age and provenance of the target materials for tektites and possible impactites as inferred from Sm-Nd and Rb-Sr systematics. *Earth and Planetary Science Letters* 60:155–177.

Taylor P. N., Moorbath S., Leube A., and Hirdes W. 1992. Early Proterozoic crustal evolution in the Birimian of Ghana: Constraints from geochronology and isotope geochemistry. *Precambrian Research* 56:97–111.

Taylor S. R. and McLennan S. M. 1985. *The continental crust: Its composition and evolution.* Oxford: Blackwell Scientific. 312 p.

Tuchscherer M. G., Reimold W. U., Koeberl C., and Gibson R. L. 2004. Major- and trace-element characteristics of impactites from the Yaxcopoil-1 borehole, Chicxulub structure, Mexico. *Meteoritics & Planetary Science* 39:955–978.

Wedepohl K. H. 1995. The composition of the continental crust. *Geochimica et Cosmochimica Acta* 59:1217–1232.

Wright J. B., Hastings D. A., Jones W. B., and Williams H. R. 1985. *Geology and mineral resources of West Africa.* London: George Allen and Unwin. 187 p.